AFML-TR-71-182

MASS-SPECTROMETRIC STUDIES OF GRAPHITE VAPORIZATION AT HIGH TEMPERATURES

Thomas A. Milne
Jacob E. Beachey
Frank T. Greene
Midwest Research Institute

TECHNICAL REPORT AFML-TR-71-182

September 1971

Approved for public release;
distribution unlimited.

Air Force Materials Laboratory
Air Force Systems Command
Wright-Patterson Air Force Base, Ohio

75

UNCLASSIFIED

Security Classification

DOCUMENT CONTROL DATA - R & D

(Security classification of title, body of abstract and indexing annotation must be entered when the overall report is classified)

1. ORIGINATING ACTIVITY (Corporate author)

Midwest Research Institute
425 Volker Boulevard
Kansas City, Missouri 64110

2a. REPORT SECURITY CLASSIFICATION: Unclassified

2b. GROUP

3. REPORT TITLE

MASS-SPECTROMETRIC STUDIES OF GRAPHITE VAPORIZATION AT HIGH TEMPERATURES

4. DESCRIPTIVE NOTES (Type of report and inclusive dates)

Technical Report (1 July 1968 to 31 May 1971)

5. AUTHOR(S) (First name, middle initial, last name)

Thomas A. Milne Frank T. Greene
Jacob E. Beachey

6. REPORT DATE	7a. TOTAL NO. OF PAGES	7b. NO. OF REFS
September 1971	64	15

8a. CONTRACT OR GRANT NO.	9a. ORIGINATOR'S REPORT NUMBER(S)
F33615-68-C-1709	
b. PROJECT NO. 7360	
c. Task No. 736001	9b. OTHER REPORT NO(S) (Any other numbers that may be assigned this report)
d.	AFML-TR-71-182

10. DISTRIBUTION STATEMENT

Approved for public release;
distribution unlimited.

11. SUPPLEMENTARY NOTES	12. SPONSORING MILITARY ACTIVITY
	Air Force Materials Laboratory Wright-Patterson AFB, Ohio 45433

13. ABSTRACT

Following a first year devoted to constructing the high-pressure sampling system, mass spectrometer and testing the effect of cold orifices on hot gases, the second year was devoted to testing and debugging the system. Equilibrium carbon species up to C_7 were observed from pyrolytic graphite Knudsen cells. The third year involved seeking a graphite cell design and heating arrangement to minimize arcing and vapor loss. The use of slotted pyrolytic graphite cells with various inserts appears to provide sufficient shielding to permit attainment of inner temperatures in the 3500°K range. Arcing could not be prevented with the RF work coil inside the vacuum system, even with the use of a step-down transformer. Hence, we have returned to the use of a current concentrator inside a Pyrex tube, with the high voltage coil outside the vacuum. This arrangement appears successful. A second task involved implementation of the data acquisition schemes--particularly time-of-arrival velocity analysis of carbon species using ion counting. It was found that both the original Nuclide ion source and a variation of it suffered from severe ion trapping, causing delayed and distorted time-of-arrival curves. A third ion source had adequate time response but substantially lower sensitivity. The behavior of several ion source configurations is described in detail as is a fast peak-switching scheme.

DD FORM 1 NOV 65 1473

UNCLASSIFIED

Security Classification

NOTICE

UNCLASSIFIED

Security Classification

14. KEY WORDS	LINK A		LINK B		LINK C	
	ROLE	WT	ROLE	WT	ROLE	WT
Free-Jets						
Graphite						
High Temperature						
Laser Heating						
Mass Spectrometry						
Mass Separation						
Molecular Beams						
Nucleation						
Thermochemistry						
Vaporization						
Velocity Analysis						
Induction Heating						

UNCLASSIFIED

Security Classification

MASS-SPECTROMETRIC STUDIES OF GRAPHITE VAPORIZATION AT HIGH TEMPERATURES

Thomas A. Milne
Jacob E. Beachey
Frank T. Greene

ABSTRACT

Following a first year devoted to constructing the high-pressure sampling system, mass spectrometer and testing the effect of cold orifices on hot gases, the second year was devoted to testing and debugging the system. Equilibrium carbon species up to C_7 were observed from pyrolytic graphite Knudsen cells. The third year involved seeking a graphite cell design and heating arrangement to minimize arcing and vapor loss. The use of slotted pyrolytic graphite cells with various inserts appears to provide sufficient shielding to permit attainment of inner temperatures in the 3500°K range. Arcing could not be prevented with the RF work coil inside the vacuum system, even with the use of a step-down transformer. Hence, we have returned to the use of a current concentrator inside a Pyrex tube, with the high voltage coil outside the vacuum. This arrangement appears successful. A second task involved implementation of the data acquisition scheme--particularly time-of-arrival velocity analysis of carbon species using ion counting. It was found that both the original Nuclide ion source and a variation of it suffered from severe ion trapping, causing delayed and distorted time-of-arrival curves. A third ion source had adequate time response but substantially lower sensitivity. The behavior of several ion source configurations is described in detail as is a fast peak-switching scheme.

FOREWORD

This report was prepared by Midwest Research Institute, 425 Volker Boulevard, Kansas City, Missouri 64110, under USAF Contract No. F33615-68-C-1709. The contract was initiated under Project No. 7360, "Chemical, Physical, and Thermodynamic Properties of Aircraft, Missile, and Spacecraft Materials," Task No. 736001, "Thermal and Chemical Behavior of Advanced Weapon System Materials." The work was administered under the direction of the Air Force Materials Laboratory, Air Force Systems Command, Wright-Patterson Air Force Base, Ohio, with Mr. Paul W. Dimiduk (AFML/LPT) as Technical Monitor.

Work conducted from 1 July 1968 to 31 May 1971 is covered. The report was released by the authors in June 1971.

The work at Midwest Research Institute, designated as Project 3228-C, was performed by Dr. Thomas A. Milne, Dr. Stephen L. Bennett, Mr. Jacob Beachey, Dr. Frank T. Greene and Mr. Gil Kitterman. Mr. Gordon Gross provided technical management while Professor Paul W. Gilles, University of Kansas, served as regular consultant.

This technical report has been reviewed and is approved.

Hyman Marcus

HYMAN MARCUS, Chief
Thermo & Chemical Physics Branch
Materials Physics Division
Air Force Materials Laboratory

TABLE OF CONTENTS

LIST OF ILLUSTRATIONS

LIST OF ILLUSTRATIONS (Continued)

LIST OF ILLUSTRATIONS (Concluded)

LIST OF TABLES

LIST OF TABLES (Concluded)

SUMMARY OF THE 3-YEAR PROGRAM

We initially approached the laboratory study of the vaporization of carbon by considering three main types of experiments. Two involved heating in vacuum with direct expansion of the carbon vapor into the mass spectrometer via a molecular beam. The third involved vaporization into a surrounding high pressure gas in a transpiration experiment with subsequent expansion of the carbon-saturated gas through a cold probe into a high-pressure, molecular-beam, mass-spectrometric sampling system. One of the vacuum experiments was to involve laser-assisted vaporization using continuous laser heating together with velocity and mass analysis of the resulting neutral species to better define the evaporation conditions. This approach, while unquestionably offering the highest "temperature" and generating the largest clusters, has not been pursued because of the ambiguity of the process of vaporization with such heating.

The high pressure gas transpiration experiment has likewise not been attempted, beyond early experiments with permanent gases which gave encouragement that cold orifices could be used without compromising adiabatic sampling of hot gases. The chief deterrents to this approach to observing carbon vaporization are the practical problems of the very short expected sampling time before physical plugging of the orifice occurs and the possible clustering of the carbon species during initial expansion due to the high pressure of the carrier gas. Nevertheless, we may well return to this method to obtain both equilibrium and evaporation data when practical temperature and pressure limits on heating carbon in vacuum are encountered due to mass transport problems.

Most of the emphasis in this phase of our studies has been on observing equilibrium carbon species from graphite Knudsen cells and freely evaporating hot graphite surfaces. The major determinant factor in the direction taken by our current vaporization studies has been the realization of the anisotropic properties of pyrolytic graphite. Following early work by Ubbelohde, et al., we have carried out experimental heatings of several configurations of Knudsen cells made from pyrolytic graphite (PG). The large electrical and thermal resistivity perpendicular to the deposited planes of PG allows one to selectively heat, and obtain vapor from, the inside of PG shielded Knudsen cells or solid inserts.

We have recently established radio frequency induction heating conditions (involving the use of a current concentrator with the work coil outside the vacuum system) which provide cell temperatures in the neighborhood of 3500°K. It is anticipated that recently completed improvements in concentrator design and cell configuration will permit still higher temperature to be achieved, but with severely reduced operating time as mass loss

increases. The high pumping capacity of our high pressure molecular beam sampling system is turning out to be useful, even in the vacuum experiments, in keeping the pressures surrounding the heated cell low.

The modulated molecular beam-mass spectrometer-data acquisition system has been thoroughly tested and an anomalous background modulation eliminated so that now we can routinely use ion counting to detect very weak phase-locked signals from large carbon clusters (C_6 and C_7 have been detected for the first time from a Knudsen cell at about 2800°K) or to follow rapid changes in intensity with time with the multichannel analyzer. The latter capability, coupled with a fast two-position peak switcher, allows us to follow the intensities of any two ion peaks during short high temperature heating excursions or to carry out neutral species velocity analysis by measuring the time-of-arrival (TOA) of chopped carbon beams.

The use of time-of-arrival (TOA) velocity analysis for the various positive ions observed in the electron impact mass spectrum of carbon vapor has an important role in interpreting the vaporization behavior of graphite. Serious ion-source time response problems have been encountered and only partly resolved in that we have to give up sensitivity to get adequate time response. Initial indications that the C_3^+ peak had major contributions from higher carbon clusters at 50 eV electron energy are now suspect.

In summary, an RF heating system, pyrolytic graphite shielded cell, high-pressure modulated molecular beam sampling system, Nuclide mass spectrometer with ion counting and analog detection, fast peak switching and time-of-arrival velocity analyses system have been designed, built, debugged and tested with permanent gases and with carbon vapor and stand ready for further elucidation of carbon vapor composition at high temperatures.

I.

INTRODUCTION

The purpose of these 3 years of study has been to develop the high-pressure, direct-sampling, molecular-beam, mass spectrometer technique for the study of carbon vaporization and to apply it to the determination of the molecular composition of carbon vapor under both "free" and equilibrium evaporation conditions at temperatures exceeding 3200°K. The ultimate goal is a characterization of vapor composition in the 1-10 atm pressure regime.

The first year's efforts were spent in designing and constructing a high-capacity, molecular-beam sampling system with a Nuclide HT-90 mass spectrometer detector. While this equipment was being assembled, experiments were carried out on the Bendix TOF mass spectrometer-molecular-beam system to ascertain the extent of cooling involved in the cold-probe sampling of hot gases. The second year's effort was devoted to tests of the new sampling system, the mass spectrometer and the carbon heating schemes and included preliminary mass spectrometric observation of carbon species up to C_7^+ in equilibrium with carbon at about 2800°K. The third year has been spent in diagnostic studies in two major areas. First, various carbon-RF heating schemes have been tried with the most promising results and future indicated for the use of a current concentrator with the high voltage work coil outside the vacuum system. Second, the Nuclide ion source as originally supplied possessed two objectionable features: background modulation and inadequate time response for TOA velocity analysis under some conditions. Modification of the original ion source and tests with a second Nuclide-supplied ion source indicates solution to both problems can be obtained with loss of sensitivity.

Since results of the first 2 years' research have been presented in detail in two annual technical reports (AFML-TR-69-227 (Ref. 1) and AFML-TR-70-192 (Ref. 2)), we repeat here only the two abstracts. A similar abstract of the third year study is also included for consistency.

A. Abstract - First Year - 1 July 1968 to 30 June 1969

In connection with our goal to extend the thermodynamics and kinetics of carbon vaporization toward the 1 atm regime, we review, briefly, related work currently under way in several laboratories. Our own first year's research is then described in terms of prospective sources of carbon vapor, the problems of cold-probe sampling of hot gases and the important continuum sampling effects of mass separation and nucleation. Studies of

cold-probe, hot-gas interaction were carried out using the Bendix TOF direct sampling system. With flames at about 2500°K time-of-flight velocity analysis indicated the possibility of serious cooling by heat exchange to the cold orifice. Better controlled experiments at 1000°, using rare gases heated in a furnace flow system, gave no definite indication that sampling was not adiabatic. Considerations of free-jet expansion behavior serve to allow estimates of the conditions of carbon vaporization at which continuum effects may become important. Continuum effects could be quite significant in laser evaporation and in free evaporation from large surfaces (~ 1 in.) above 3000°K. A new, high-pumping speed, three-stage, differentially pumped, modulated-beam, direct sampling system is described. Beams are detected by a Nuclide mass spectrometer with several data acquisition options. The work planned for the second year emphasizes techniques of fast data acquisition and continuum sampling effects with carbon vapor.

B. Abstract - Second Year - 1 July 1969 to 30 June 1970

The progress in a second year of study of the thermodynamics of carbon vapor is reviewed. The status and preliminary performance of a high-capacity, three-stage, high pressure sampling system--Nuclide HT-12-90 mass spectrometer detector and data acquisition system (including time-of-flight velocity analysis of beam neutrals) is presented. Beam system calibrations with Ar, N_2 and Ag indicate partial pressures of about 1×10^{-10} to 1×10^{-8} atm (depending on background) can be detected from a Knudsen cell with a 0.040 dia orifice placed 56 cm from the ion source. A troublesome feature of the present ion source is that some modulation of background peaks occurs in the presence of modulated beams. A series of attempts to heat graphite in vacuum to temperatures greater than 3000°K are described. Best results are obtained with slotted pyrolytic graphite cells but arcing still limits heating to 3000° to 3100°K. Carbon species through C_7 have been observed from a pyrolytic graphite Knudsen cell. The C_1 to C_5 data agree well with literature values, at the two temperatures of 2800°K and 2630°K. A correlation of dimer formation versus expansion conditions for a number of gases, studied to date, indicates that nucleation cannot be ruled out in high-pressure Kundsen cells or laser heatings.

C. Abstract - Third Year - 1 July 1970 to 30 April 1971

During the third year, two tasks were predominant. The first involved seeking a graphite cell design and heating arrangement to minimize arcing and vapor loss. The use of slotted pyrolytic graphite cells with various inserts appears to provide sufficient shielding to permit attainment of inner temperatures in the 3500°K range. Arcing could not be prevented with the RF work coil inside the vacuum system, even with the use of a step-down

transformer. Hence, we have returned to the use of a current concentrator inside a Pyrex tube, with the high voltage coil outside the vacuum. This arrangement appears successful. The second task involved implementation of the data acquisition schemes--particularly time-of-arrival velocity analysis of carbon species using ion counting. It was found that both the original Nuclide ion source and a variation of it suffered from severe ion trapping, causing delayed and distorted time-of-arrival curves. A third ion source had adequate time response but substantially lower sensitivity. The behavior of several ion source configurations is described in detail as is a fast peak-switching scheme.

II.

PRESENT STATUS OF KNOWLEDGE OF CARBON VAPORIZATION

Past and current work related to an understanding of the vaporization behavior of carbon has been reviewed in previous reports (Refs. 1 and 2). Currently, we know of no other active research effort except that using laser evaporation aimed at the mass spectrometric characterization of the free or equilibrium evaporation of graphite at temperatures beyond 3200°K. Impressions gained from a recent meeting (Ref. 3) of workers involved in graphite ablation studies are: (1) the triple point temperature of carbon is still uncertain by hundreds of degrees although a pressure of about 100 atm seems well established. (2) Model calculations of carbon vapor composition based on experimental and computed heats of association and statistical mechanical partition functions using estimated or incomplete molecular parameters are sufficiently uncertain (or flexible) to permit agreement with the whole range of proposed triple-point temperatures and with observed ablation test behavior. In particular, the importance of clusters beyond C_3 is still an open question at pressures of 1-100 atm. (3) A large uncertainty still exists in both the heat of formation of C_3 and in the partition functions needed to extrapolate low-temperature measurement results to much higher temperatures. This is particularly serious since most estimates of higher carbon cluster properties are based crucially on C_3 properties. (4) The concept of free evaporation and the ability to measure operationally meaningful evaporation coefficients for different species from graphite is questionable. This problem is more serious the higher the rate of evaporation, because of the heterogeneous nature of graphites, the observed highly preferential mode of evaporation of binder and filler and the probable onset of gas-gas collisional reactions at high rates of carbon loss. (5) Direct loss of macroscopic particles from hot graphite may constitute an appreciable fraction (more than half) of the total weight loss when graphite is heated in vacuum, inert gas or air.

It is the continued goal of our research to try to directly characterize the mole fractions of carbon species from Knudsen cell evaporation or "free" surface evaporation in vacuum, to as high a temperature as our heating techniques will allow. It is unlikely that unambiguous third-law heats can be deduced from such ratios in view of the lack of knowledge of the proper parameters to use in calculating the entropy of C_3 and, especially, higher clusters. Second-law heats may become ambiguous due to the onset of continuum expansion reactions in the gas phase and due to temperature dependent ionization cross sections. Thus, our minimum goal is to arrive at the best direct estimate of vapor phase species mole fractions (vapor molecular weight) by direct mass spectrometric observations at temperatures as close to the conditions of interest as can be physically realized.

Table I presents the species studied and temperatures achieved in past free and equilibrium vaporization work using mass spectrometric detection. Based on these studies, we plan to emphasize the species beyond C_3 and temperatures beyond 3200°K (hopefully approaching 3700°K).

TABLE I

MAXIMUM TEMPERATURES REACHED IN CARBON STUDIES

Worker	Kind of Graphite and Heating Method	Equilibrium or Free Evaporation	Species Studied	Maximum Temperature Reached
Clarke & Fox (Ref. 4)	UTG fine crystal, resistance	Free*	Wt. loss and heat loss	3410°K
Steele (Ref. 5)	RG-504, Ta sleeve Induction	Equilibrium Free	C_3^+ C_1^+, C_2^+, C_4^+	3200°K $\leq$ 3000°K
	RG-504, Ta sleeve Induction	Free	$C_1^+ \ldots C_7^+$, C_9^+, C_{10}^+	~ 2900°K
	RG-504, Ta sleeve Induction	Free	C_1^+, C_4^+, C_5^+, C_6^+	3200°K
Wachi & Gilmartin (Ref. 6)	Conventional Graphite, resistance	Free	C_1^+ - C_5^+	3000°K
	PG, resistance	Free	C_1^+ - C_5^+	3260°K
Williams (Ref. 7)	Graphite, resistance in Ta tube	Equilibrium	C_1^+ - C_5^+	3000°K
Zavitsanos (Ref. 8)	PG, induction	Equilibrium	C_1^+ - C_4^+	3003°K
Ubbelhode (Ref. 9)	PG, induction	Neither*	-	2900°K (3700°K in Helium)
Storms (Ref. 10)	Various Carbides	Neither*	-	to 4000°K
This Work	PG Knudsen Cell, induction	Equilibrium	C_1^+ - C_7^+	2800°K
	PG Knudsen Cell, induction	Equilibrium*	-	3500°K

* No mass spectrometric characterization of vapor.

III.

RESULTS AND PROBLEMS WITH THE NEW SYSTEM

The details of our past year's efforts plus a review of present status and performance of the experimental equipment and techniques are given in the following four sections.

A. Beam Sampling Equipment, Techniques, Performance

The three-stage, differentially-pumped, molecular-beam inlet system is described in detail in Ref. 1, p. 35, and remains substantially unchanged. The beam swallowing ion pump, situated directly on top of the ion source, turned out to offer little advantage in present experiments and has been replaced with a window which serves for optical beam-alignment purposes.

System performance with permanent gases has been documented in Ref. 2, p. 8. All modulated beam work has used the components listed on p. 35 of Ref. 2. The motor has operated well between the limits of 10 and 300 cycles/sec. A variety of chopping disks have been used for phase-sensitive detection and time-of-flight velocity analysis. Phase shift measurements of most probable velocity have not been used. The two chopping schemes adopted for carbon vapor work, together with the detection equipment in block diagram, are shown in Figures 1 and 2.

A special feature of the reversible-counting, phase-sensitive detection scheme (lower half of Figure 1) which has been developed by Greene, should be mentioned. The narrow, pulsed signal from the photocell is delayed and shaped in the first pulse generator in order to produce a square wave of nearly equal on and off times and at the frequency of beam chopping. This square wave is phased with the beam chopping and controls the add/subtract mode of the counter or multichannel analyzer. Because it is difficult to make the add/subtract intervals precisely equal and to keep them in-phase with the chopping, the frequency is doubled and a second pulse generator is used to gate the counting system on. For each square wave generated by the first pulse generator, two short pulses are formed which then trigger the second pulse generator. The second pulse generator then produces pulses which are slightly shorter than the add/subtract time intervals. These pulses gate on the single channel analyzer during both the add and subtract phase so that statistical variations in pulse width or timing will average out precisely over long times.

During the past year we modified the photocell holder-chopper design so that both the light and molecular beams were chopped simultaneously.

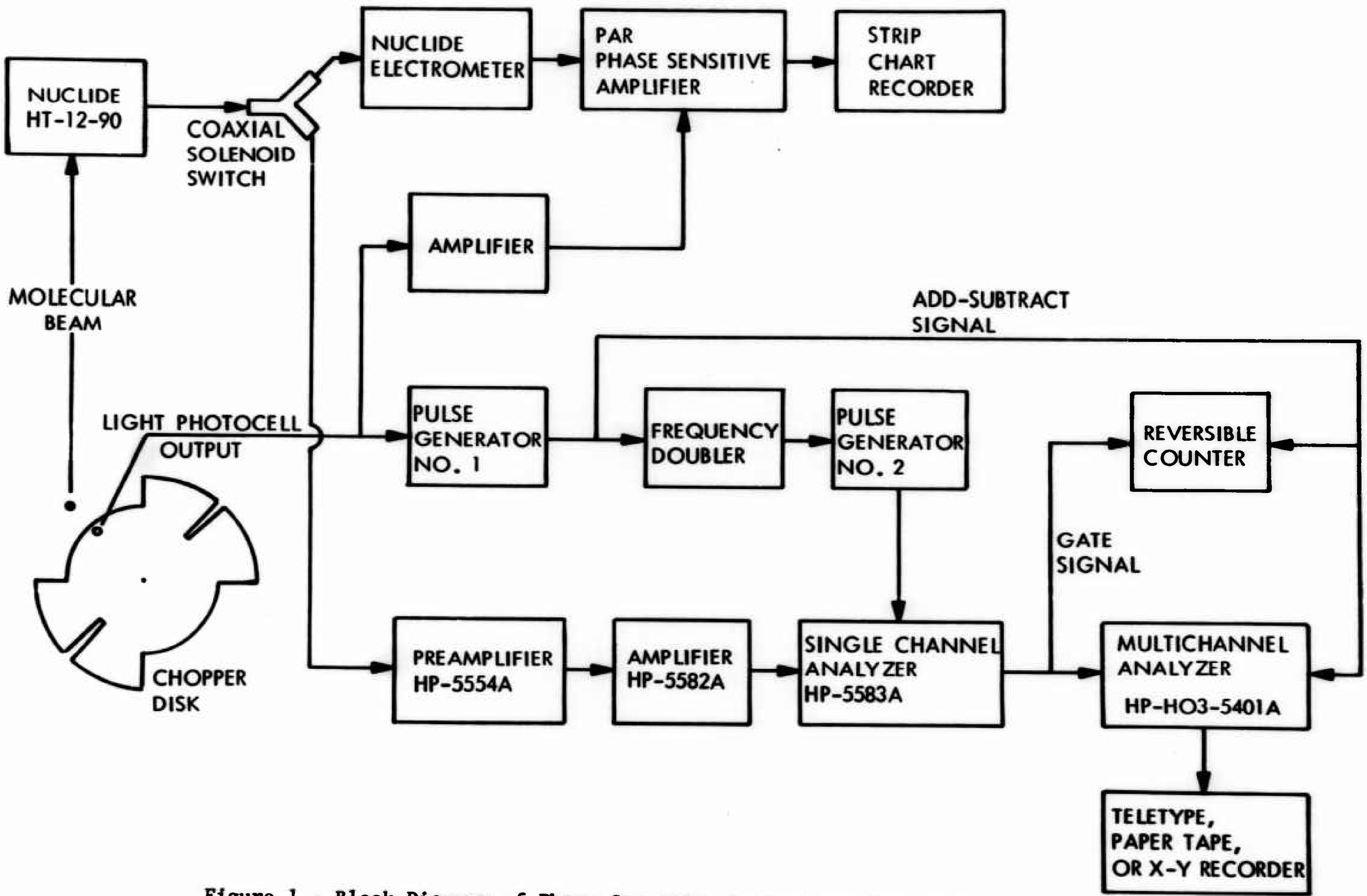

Figure 1 - Block Diagram of Phase Sensitive Detection Scheme Using Either Analog Detection or Direct Ion Counting

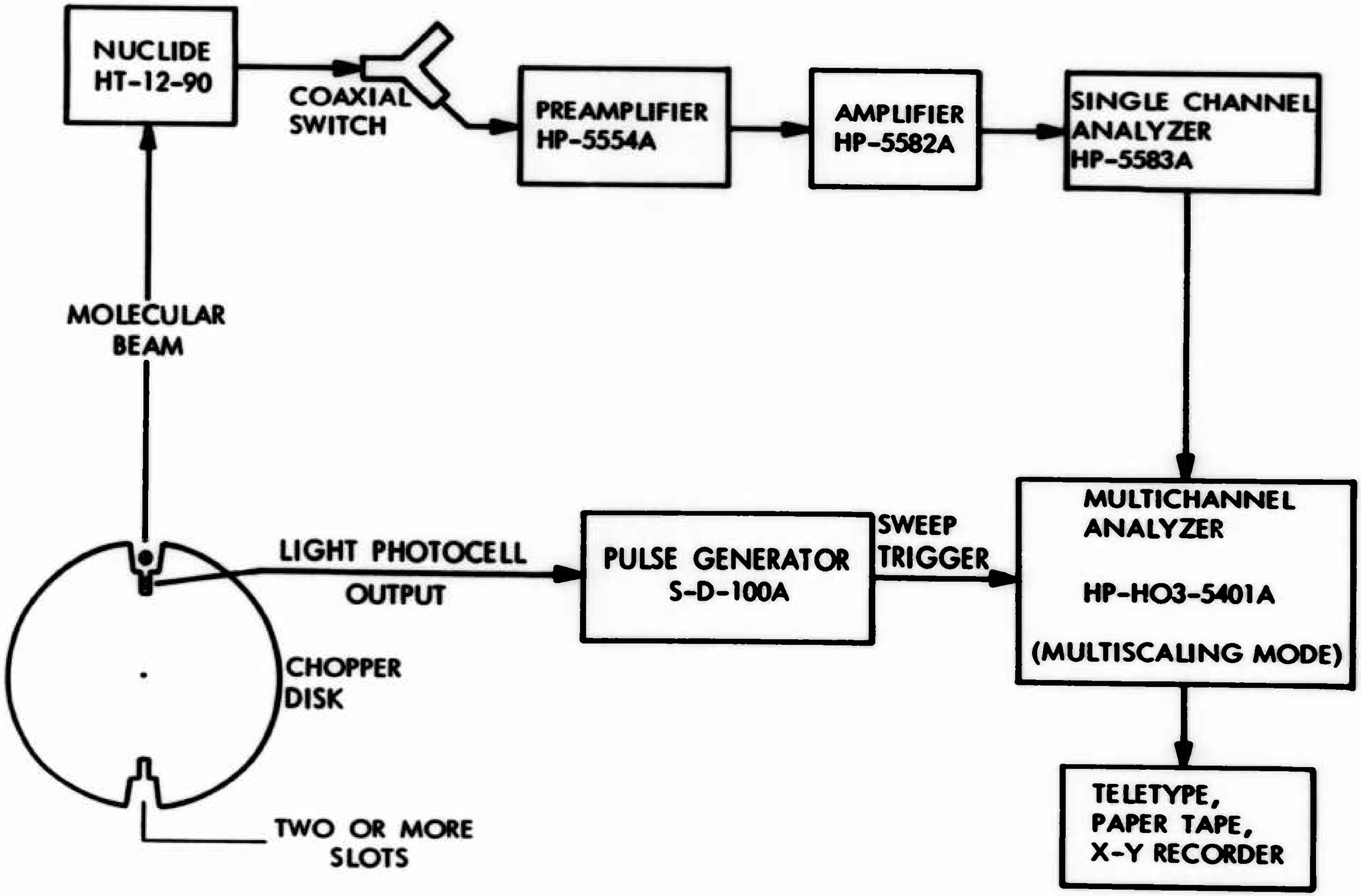

Figure 2 - Block Diagram of Time-of-Arrival Velocity Analysis Scheme Using Direct Ion Counting

(See Figure 2.) This reduces the error in making absolute velocity measurements and in fact may avoid the necessity of using motor reversal to cancel out relative light and beam chopping geometry. Time response of the photocell system still needs improvement to remove uncertainties associated with triggering the multichannel analyzer in the multiscaling mode.

The chopper design shown in Figure 2 is chosen for time-of-arrival velocity analysis of carbon species under near-effusive flow, e.g., C_3 at 3000°K. Results and problems with such measurements are discussed in detail below.

B. Mass Spectrometer-Data Acquisition System

1. Nuclide general performance. Apart from ion source problems discussed in the next paragraph, the Nuclide HT-12-90 has performed reasonably well. Although the source high voltage supply malfunctions every month or so, at other times the machine will remain focused on a given ion for 24 hr. or longer. (With ion extraction and detector slits wide open for maximum transmission.) Typical operating data are shown in Ref. 2, pp. 9-12.

2. Background modulation. A very serious problem was encountered in early modulated-beam tests in the second year. It was found that with the original ion source supplied with the instrument, presence of a modulated beam in the ion source caused a modulation of all background ions, the amplitude and phase of which varied with ion source parameters, particularly repeller voltage (Ref. 2, p. 12). During the past year, while the Nuclide was in use by another project, a simple modification of the ion source shown in Figure 3, p. 13 of Ref. 2 seems to have eliminated this particular problem to within our present limits of detection. The following excerpt from a recent project report (Ref. 11) summarizes the reasoning and modifications.

"One possible explanation for the nonlinearity effect (background modulation) invokes the electrostatic focusing of the electron beam by the ions formed from species in the beam. It therefore seemed possible to reduce or eliminate the nonlinearity by sufficient collimation or focusing of the electron beam so that the electrostatic focusing would be insignificant. This could be accomplished by magnetic focusing, by collimation of the electron beam, or by reducing the electron density so as to reduce spreading of the beam.

"Magnetic focusing seemed simplest and was attempted first. Magnets were simply introduced into the ion source with the field directed along the axis of the electron beam. Several configurations were tried. The extent of nonlinearity was reduced by approximately one order of magnitude, but a significant amount remained. The ionization efficiency of the source was not improved.

"The collimation of the electron beam was then improved by the reduction of the size of the aperture, which, together with the filament, defines the beam (in this ion source, the electron beam does not have a second collimating aperture and the beam is therefore very poorly collimated). This also should reduce the electron density in the beam. A number of combinations of filaments and apertures were tried."

In the course of seeking to eliminate the background modulation phenomena a number of ion sources and modifications have been tested. Approximate sensitivities of each source were measured by observing the signals from well collimated supersonic beams of N_2. Background modulation tests were also performed although no systematic variation of ion source parameters was involved. The ion sources tested are listed in Table II together with approximate relative sensitivities, and the relative extent of background modulation. (See Appendix for observations furnished by Nuclide Corporation.)

3. Ion counting parameters. One of the key design capabilities of our carbon-vaporization, beam-sampling, mass-spectrometer system involves the use of ion counting and subsequent multichannel scaling to observe the time of arrival of mass spectral ions from chopped beams of carbon vapor. Three principal features of such analysis are: (1) the detection of fragment ion contribution to a given species, C_n^+, by time-of-arrival curve analysis under effusive, or near-effusive conditions; (2) the use of most-probable-velocities of species as a measure of source temperature; and (3) the earliest detection of continuum expansion effects through alteration of relative velocities of different species and the subsequent correction of observed species ratios for mass separation. In this section are presented the results of preliminary tests involving ion-counting.

The Hewlett-Packard ion-counting system, consisting of a charge-sensitive preamplifier (Model 5554A), a linear amplifier (Model 5582A) and a single channel analyzer (Model 5583A) feeding a multichannel analyzer (Model 5401A) performed generally in the expected manner. For general counting, with best signal-to-noise performance, the multiplier dynode string current was set at 0.4 mA (a gain of about 1 x 10^6), the preamp at 1,000 mV/picocoulomb and voltage gain x 2, the amplifier in the double-delay-line mode (1,000-nsec delay with integration of 1 μsec to 5 μsec and gain of 18, and the single channel analyzer Emin set at 1 V. Pulse height analysis revealed a large number of pulses in the millivolt range reaching the single channel analyzer. These were easily suppressed. With the RF generator operating, a large sine wave at the generator frequency was present on the collector and could only partly be discriminated against in the above pulse shaping mode. Much better results were obtained using double RC differentiation and integration with 0.1/0.1/0.1 μsec settings on the linear amplifier, a gain of 8 and Emin of 1.00 V. In this mode the RF interference was completely suppressed with little loss in ion pulse count rate.

TABLE II

COMPARISON OF RESPONSE TO MODULATED BEAMS OF SEVERAL ION SOURCES

Description of Ion Source	Typical Phase Locked Ion Intensity from 1 Atm N_2 Beam. 0.004 In. Orifice 50 eV, 1 mA Emission (arbitrary units)	Typical Approximate Extent of Background Modulation (percent of peak dc.) (Highly variable with ion source parameters)
Original source as supplied by Nuclide. Nonmagnetic (see Figure 3, Ref. 2) single electron beam aperture. 0.025 x 3/16 in. (Source No. 1)	100	20
Source No. 1 with internal magnets added.	5	1.5
Source No. 1 with electron beam aperture reduced to 1/32 in. on inside of ion box.	47	≤ 0.1
Source No. 1 with electron beam aperture reduced to 1/64 in. on outside of ion box.	4 (at 2 mA)	≤ 0.1
Source No. 1 with electron beam aperture reduced to 1/32 in. on outside of ion box. (Source No. 2)	12	≤ 0.1
Nuclide magnetic ion source.	0.7	1
Nuclide double aperture non-magnetic source (Source No. 3)	0.6	≤ 0.1

In either mode it was difficult to count from the 16th dynode (while reserving the collector for simultaneous analog detection). Noise was always much greater at the poorly shielded 16th dynode and was intolerable during RF heating. We thus employed a solenoid operated, coaxial switch for rapid conversion from ion counting to electrometer output. During the work on the ion-counting setup, the previously reported 60-cycle modulation on all ion peaks was effectively eliminated, following changes in the emission current regulator section, suggested by Nuclide personnel.

During the most recent ion-counting experiments with induction heating, RF interference was a serious problem. A substantial fraction of ions were not counted when discrimination levels were set sufficiently high to eliminate the RF noise. It turned out that multiplier gain had decreased about a factor of 5 (for a given dynode string setting) during the course of time and several exposures to air during changes in ion-source configuration. The gain was thus only marginal for multichannel analysis of time-of-flight behavior and seemed inadequate for the use of reversible ion counting in phase-sensitive detection on carbon clusters. Dynode replacement will correct this problem.

4. Ion source time response. Demonstration of adequate time response of the ion source to faithfully record the time of arrival of chopped beams of carbon clusters and permanent gases was undertaken following the selection of noise free counting conditions. Detailed measurements were made with three ion-source configurations and the results are presented separately, followed by a summary of the present state of our capability.

a. The first studies used the unmodified ion source originally supplied by Nuclide (Source No. 1) and described in Ref. 2, p. 13. A two-toothed chopper was used, with a narrow slot in one of the teeth. The chopper was driven at 50 cycles/sec. A photocell, which responded to light pulses from the large open slots, was used for triggering the multichannel analyzer in the multichannel scaling mode. Having had previous indications of slow response of the ion source to changing signal levels, we first qualitatively examined the shape of the square wave produced by the two large teeth on the chopping disk.

First, it was found that at emission currents of 0.5 mA or greater and at 0 repeller and 50 eV electron energy, the square wave was badly distorted. At lower electron energy the situation was worse while at positive repeller voltages it was improved. At 0.2 mA emission, good square waves were obtained at 18 to 50 eV and 0 repeller voltage but +4 V on the repeller now caused distortion. Some of these features are shown in Figure 3. Shown in Figure 4 is the time behavior of 43^+ (presumed to be a background peak) with and without the presence of a strong modulated N_2 beam in the ion source. The extent and peculiar time behavior of this background modulation is apparent. Under the ion source conditions used, the background modulation was in phase with the beam, although this was not always the case.

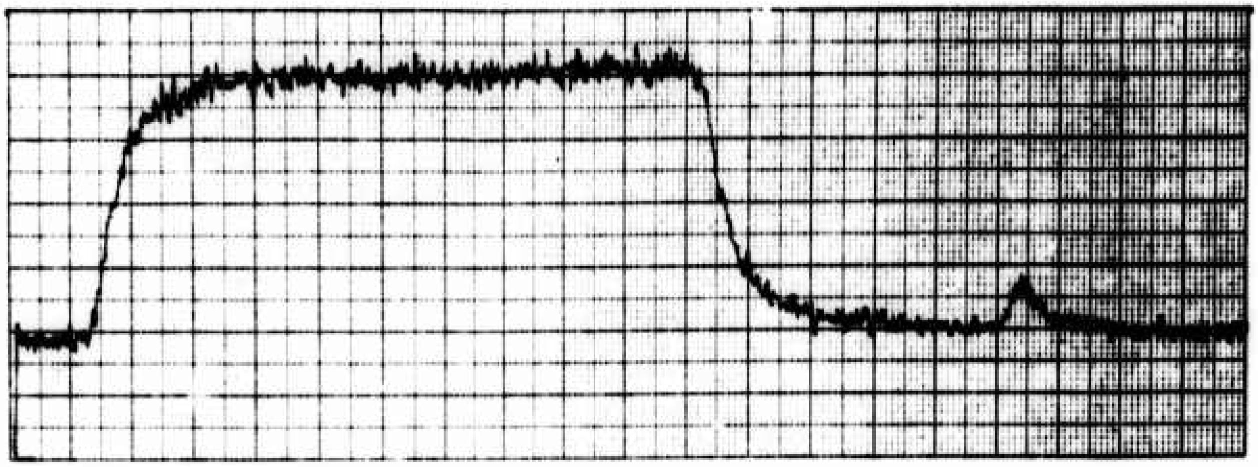

(a) Emission 1 mA, Electron Energy 50 eV, Repeller Voltage 0

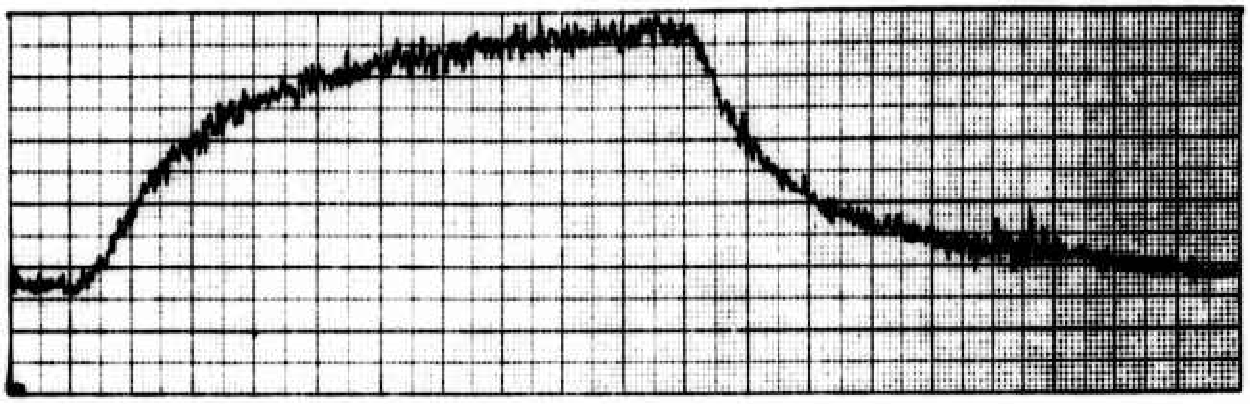

(b) Emission 1 mA, Electron Energy 20 eV, Repeller Voltage 0

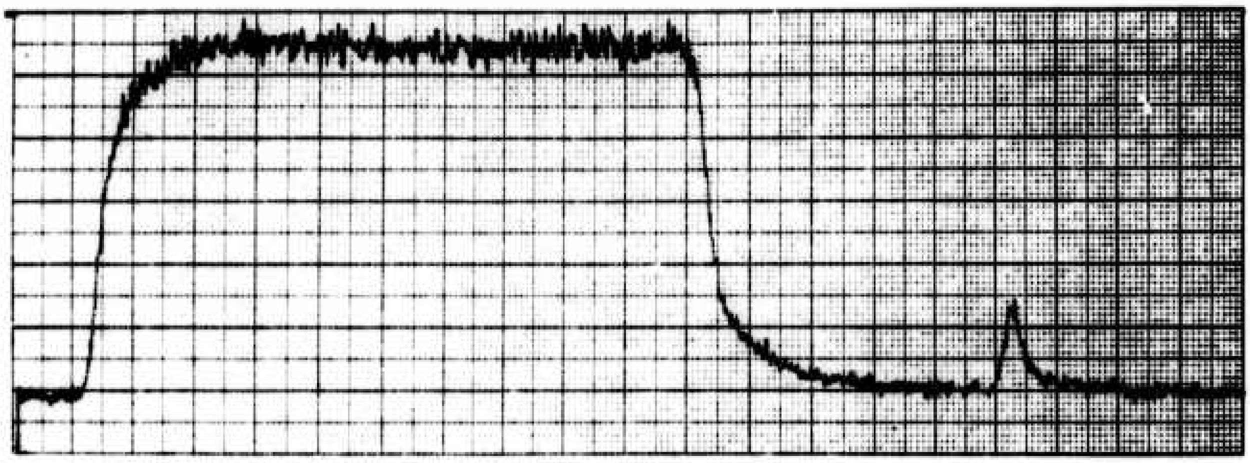

(c) Emission 1 mA, Electron Energy 50 eV, Repeller Voltage + 4 V

(d) Emission 0.2 mA, Electron Energy 20 eV, Repeller Voltage 0

Figure 3 - Effect of Emission Current, Electron Energy and Repeller Voltage on Chopped Beam Wave Forms, 29^{+} From a 1 Atm N_2 beam. Chopping rate 100 cycles/sec. Ion Source No. 1.

(a) 29^+ From N_2 Beam, 1 mA Emission, 0 Repeller

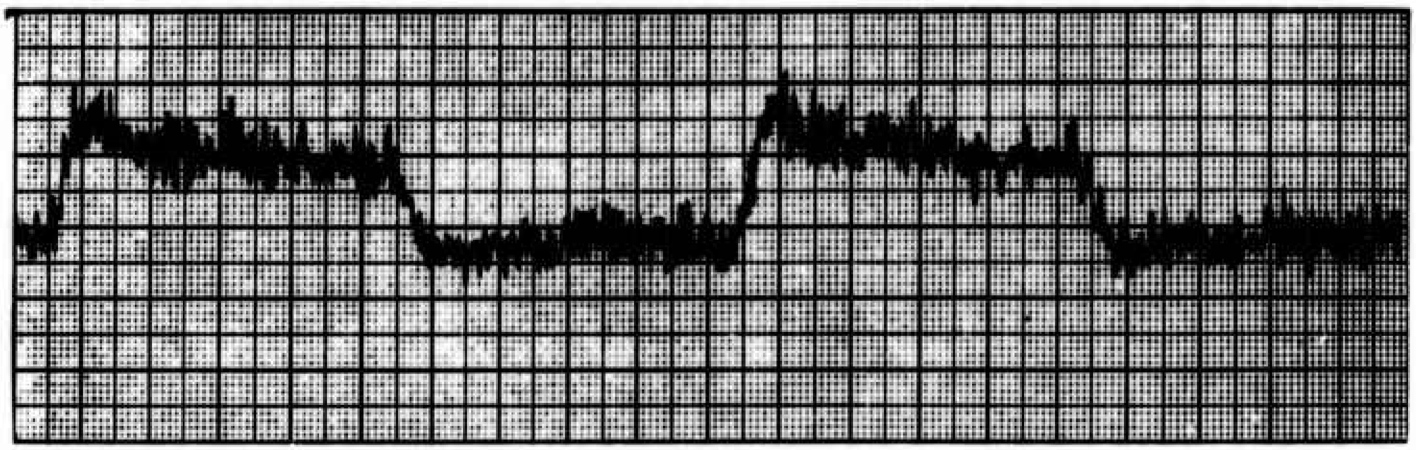

(b) 43^+, 1 mA Emission, 0 Repeller

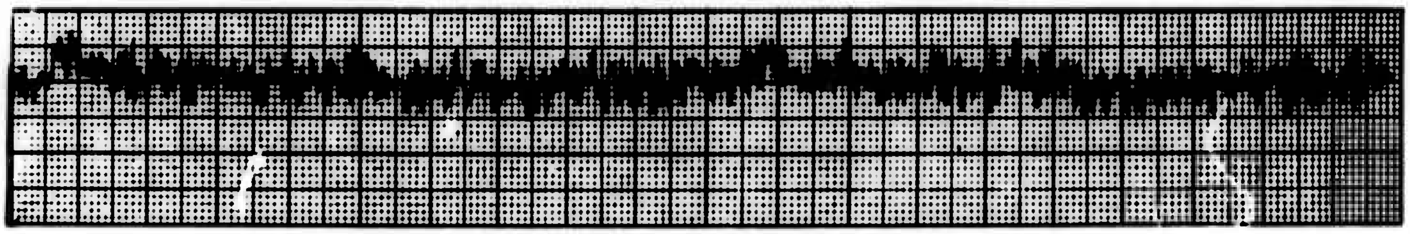

(c) 43^+, 1 mA Emission, +4 V Repeller

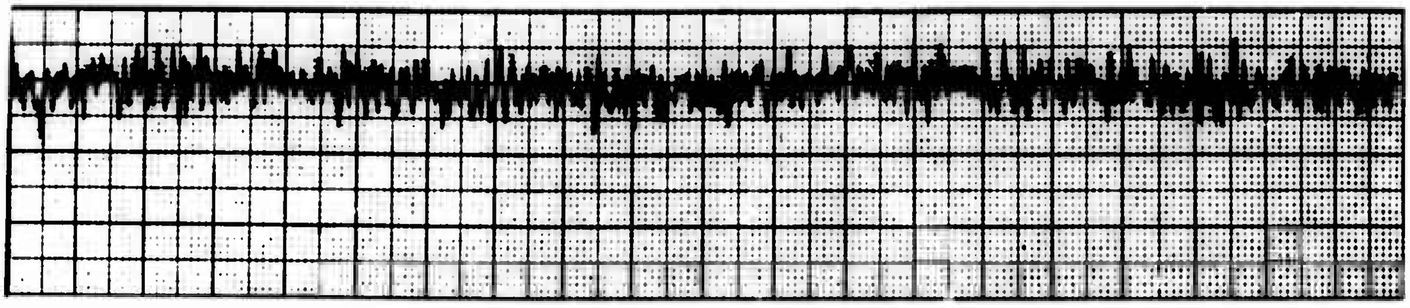

(d) 43^+, 0.5 mA Emission, 0 V Repeller

Figure 4 - Effect of Emission Current and Repeller Voltage on Modulation of a Hydrocarbon Background Peak in the Presence of a 1 Atm N_2 Beam. Chopping rate 100 cycles/sec. Ion Source No. 1.

Further tests were carried out at 0.2 mA emission current and 0 repeller voltages (other source parameters set for maximum beam intensity). Although we expected a counting rate limitation of something like 500,000 counts/sec due to the 5 mc discrimination capability of the pulse shaping train (using double delay line pulse shaping) serious problems were encountered at considerably lower count rates at the dynode string current of 0.4 mA (gain: 10^6) and the settings listed above. The first indication of trouble was a distortion of the square wave shortly after the beam came on. By carrying out measurements at tenfold lower multiplier gain it was established that the distortions correlated with multiplier output current rather than counting rate. Additional tests by another project, in which the preamplifier gain was decreased to 10 mV/picocoulomb and the amplifier gain correspondingly increased, revealed that it was the preamplifier output that was in fact overloaded. Noise discrimination was not affected by the change which permitted count rates of 10^5/sec to be used without noticeable distortion (using double RC integration and differentiation).

Using ion source conditions which appeared to give fast response to the square wave chopping, the ion intensity peak shapes produced by molecules from the single narrow slot were studied for argon and N_2 beams as a function of slit geometry, chopping frequency, pressure, electron energy and nature of the beam ion. The most severe test of time response involved supersonic beams from 0.1 to 1.0 atm source pressures, since beam velocities were highly monochromatic as a result of the free-jet expansion. Time-of-arrival (TOA) profile half widths varied with chopping speed in the expected manner. Chopping frequencies of 200 cycles/sec or greater were needed to make half widths independent of frequency for the geometry used. As pressure was reduced, half widths increased, the curves became progressively more asymetric and the most probable arrival time increased, as expected for the transition to effusive flow. Cluster-ion pulses, 56^+ in N_2 and 80^+ in argon, were narrower than for monomer, with 120^+ narrower than 80^+. Comparison with computer predictions based on expected beam velocity distributions could be reliably made only at the two extremes of either effusive flow or high Mach-number expansions, since velocity distributions are uncertain in the transition flow regime.

A problem with the beam geometry, as it affects the shutter function at the chopper, occurs in the case of free-jets from orifices smaller than the skimmer. Our initial measurements were made from 1 atm gas expanding through 0.004 in. dia orifices. A 0.040 in. dia skimmer and a 0.080 in. hole in the Nuclide shutter-plate completed the beam collimation. When it was assumed that the free-jet filled the entire skimmer uniformly (orifice-to-skimmer distance about 9/16 in.) the measured TOA curves were found to be substantially narrower than predictions. Use of a wider skimmer gave broader TOA curves but still they were narrower than predictions. Furthermore, as source pressure decreases, the actual beam width at the chopper necessarily

decreases. To achieve a pressure independent, unambiguous shutter function, we increased the orifice diameter to 0.040 in. and lowered source pressure to 1/10 atm to keep the same source Knudsen number and hence free-jet expansion conditions. Parameters affecting TOA curve predictions are shown in Table III.

Time-of-arrival curves suitable for computer comparison were obtained under three conditions: 1/10th atm N_2 (0.040 in. orifice); 1/10th atm argon (0.040 in. orifice); and 0.15 torr N_2 (0.004 in. orifice). The high pressure N_2 curves were significantly narrower than predictions based on Anderson and Fenn's (Ref. 12) criterion for terminal Mach-numbers and use of a γ of 7/5. The argon curve was in good agreement with predictions. Most-probable-velocity differences between argon and N_2 free-jet beams agreed well with theory as did the time differences between high pressure and effusive beams of N_2.

Figures 5 and 6 show results from N_2 expanding at 1 torr and 0.15 torr, respectively, both near effusive-flow conditions. At 1 torr the ratio of mean free path to orifice diameter (0.004 in. orifice) is about 0.5, yet substantial narrowing of the peak is apparent compared to Knudsen predictions and experiment, as is shown in Figure 6. The agreement at 0.15 torr source pressure was encouraging. Figure 7 compares the experimental curves for N_2 at 1.0 versus 0.15 torr source pressure. Note the substantial change in peak arrival time at 1.0 torr.

The effect of electron energy on time-of-arrival peak shape was of concern for the anticipated low ionization voltages (17 eV) to be used with carbon studies. Measurements with supersonic N_2 beams showed no broadening of TOA curves from 50 eV down to 16 eV. All the effusive measurements were made only at 50 eV, however. These results satisfied us at that time, that the ion source was responding adequately for the anticipated studies with carbon, involving near-effusive flow. C_1 and C_3 time-of-arrival profiles were taken with this source before it was modified (see below).

b. Following the simple modifications of the original ion source to eliminate the background modulation phenomena, we repeated tests of the source time response (Source No. 2). These tests all involved parent ions from intense supersonic argon and N_2 beams. At this point in time we did not suspect that beam intensity might be an important variable or that fragment ions might behave differently than parent ions.

TABLE III

VALUES OF BEAM PARAMETERS USED IN COMPUTER PREDICTIONS OF TIME-OF-ARRIVAL BEHAVIOR

Gas	Pressure (atm)	Assumed Mach-Number	Assumed (γ)	Final T (°K)	Calculated Beam Width at Chopper (in.)	Distance Orifice to Detector* (cm)	Orifice Diameter (in.)
N_2	0.1	9.55	7/5	15.6	0.056	66.8	0.040
N_2	0.01	4.95	7/5	50.8	0.056	66.8	0.040
Ar	0.1	21.6	5/3	1.9	0.056	66.8	0.040
N_2	Effusive	0	-	300	0.035	66.8	0.004
C_1	Effusive	0	-	2700	0.071	75.2	1/16
C_3	Effusive	0	-	2700	0.071	75.2	1/16

* Chopper-to-detector is 41 cm.

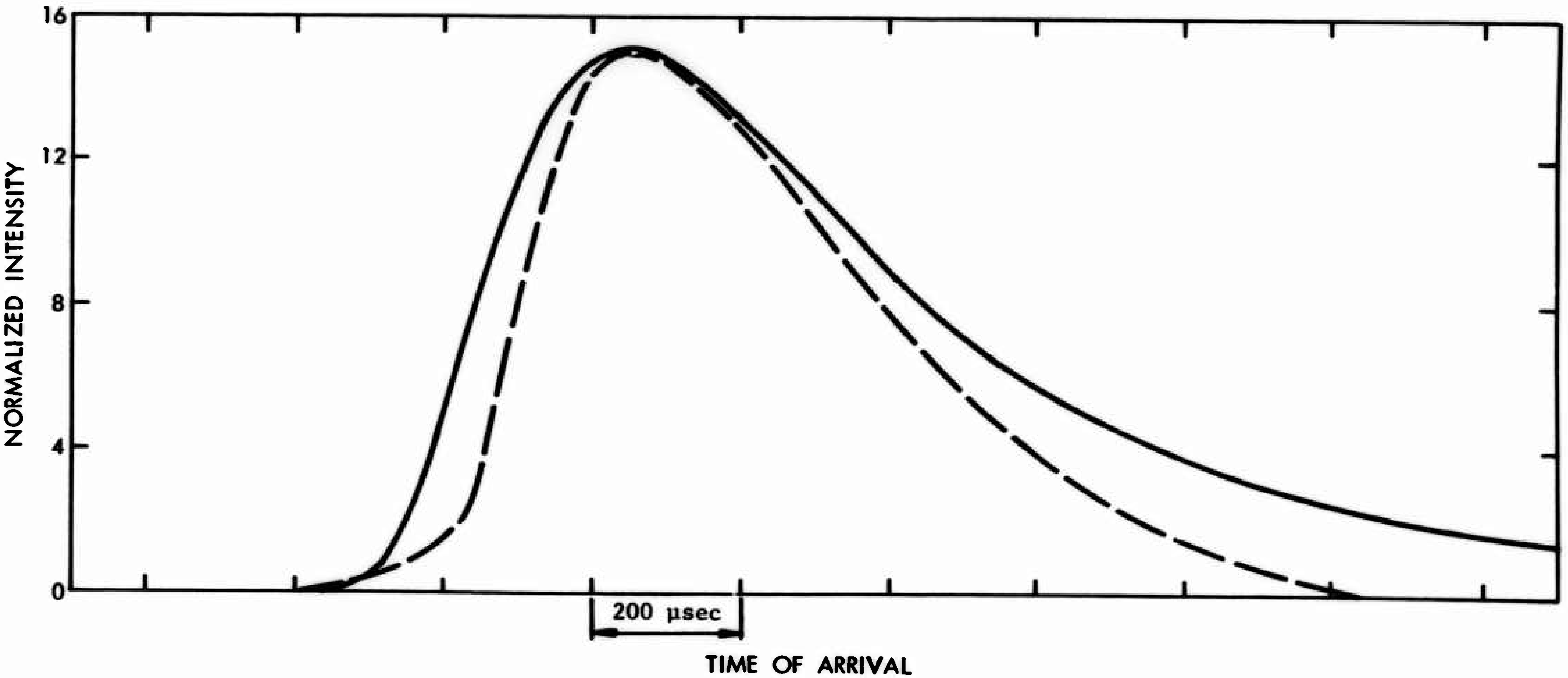

Figure 5 - Time-of-Arrival Behavior of a Chopped, Near-Effusive Beam. N_2 at 1.0 torr, 0.004 in. orifice. Solid curve is calculated for effusive flow. Time scale is shifted to make peaks match. Ion Source No. 1. Electron energy 50 eV, 0.2 mA emission.

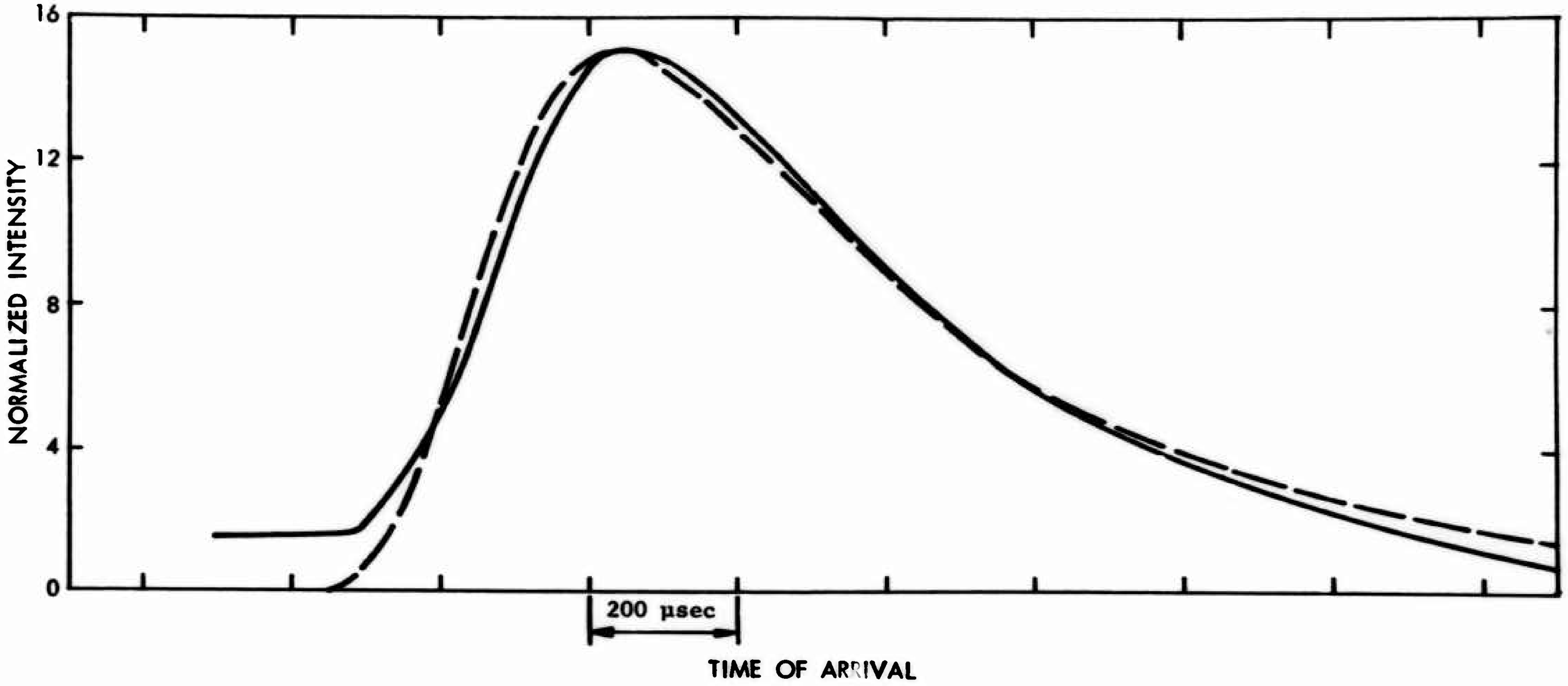

Figure 6 - Time-of-Arrival Behavior of a Chopped, Near-Effusive Beam. N_2 at 0.15 torr, 0.004 in. orifice. Dashed curve is calculated for effusive flow. Time scale shifted to make peaks match. Ion Source No. 1. Electron energy 50 eV, 0.2 mA emission.

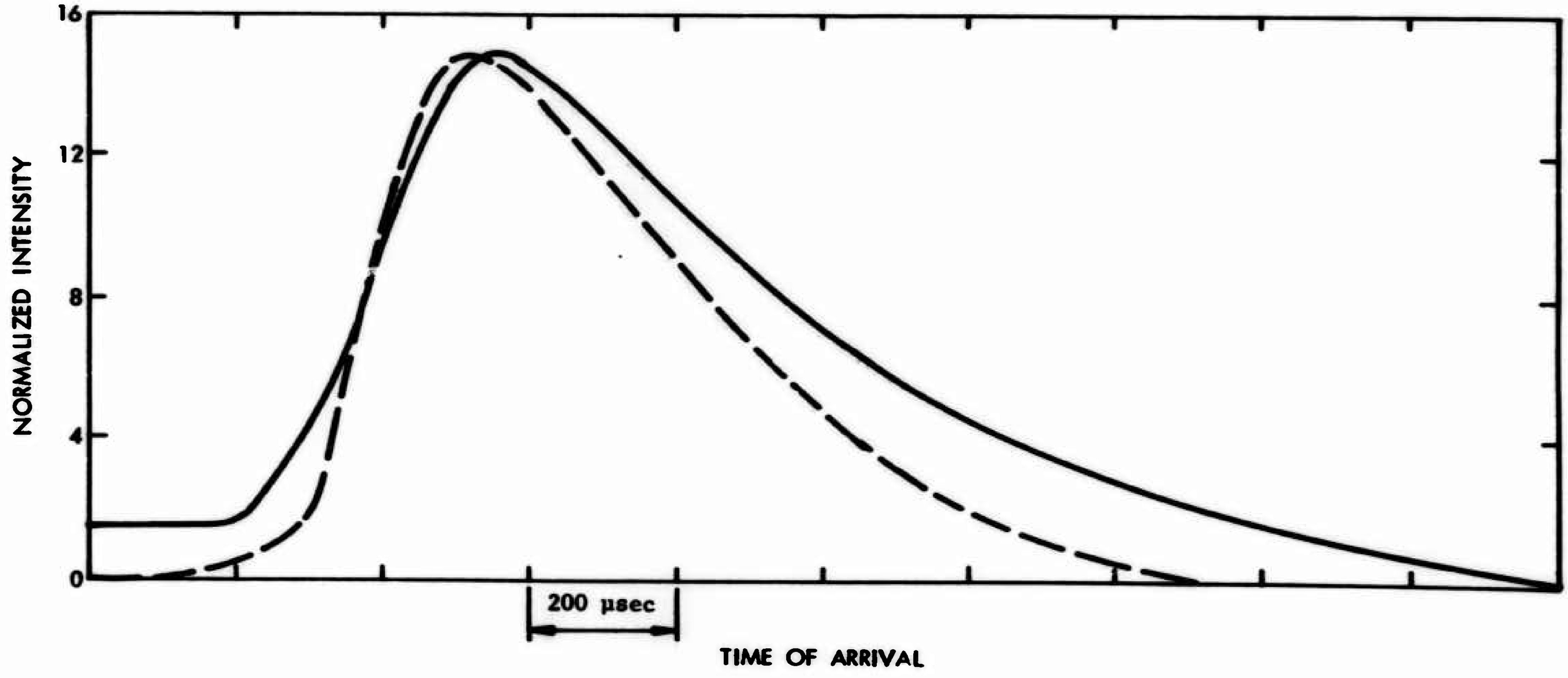

Figure 7 - Time-of-Arrival Behavior for Chopped, Near-Effusive Beams. N_2 at 1.0 torr (solid curve) and 0.15 torr, 0.004 in. orifice. The most probable arrival time difference of about 50 µsec represents about a 5% speed-up in velocity from 0.15 to 1.0 torr. Ion Source No. 1. Electron energy 50 eV, 0.2 mA emission.

The time response of the modified ion source was checked under the chopping conditions to be used in the next graphite vaporizations. Points to be established included: (1) demonstration of agreement between calculated and measured time-of-flight profiles for a high Mach-number, permanent-gas beam; (2) demonstration that ion source time response was unaffected by emission current or electron energy variation over the range of interest to carbon; and (3) establishment of the maximum counting rates that could be used without distortion of the time-of-flight data. The results of these tests are summarized in Tables IV and V and Figures 8 and 9.

From Table IV it is seen that electron energies down to about 16 eV did not noticeably affect the time response of the ion source, nor did emission current variations from 0.5 to 2.0 mA. Figures 8 and 9 show that excellent agreement was realized between predicted and measured time-of-arrival for argon and N_2 beams of high Mach number. Table V shows that at high counting rates, distortion occurred with a consequent serious broadening of the time-of-arrival curves. Such limitations on counting rate, of whatever origin, will be considered when intense carbon beams are encountered.

Following these tests, more time-of-flight measurements were made on C_1, C_2 and C_3, mainly at 17.0 and 50.0 eV. The behavior, which included shifts to later times and broadening at 50 eV (see below) could be explained on the basis of contributions from fragmentation at the higher voltages. However, when electron energy was increased to 100 eV, the C_3^+ curve was delayed to such an extent as to lack credibility. Furthermore, the TOA curves were greatly delayed when emission current was decreased. As a result of this behavior, which could hardly be attributable to simple fragmentation contributions alone, we undertook a broader series of tests of the time response of the modified ion source, including such variables as beam intensity, fragment versus parent ion behavior and other ion-source parameters.

Beams of various gases were expanded through a 0.040 in. orifice with the same beam system and chopper geometry as used in the carbon studies. Time-of-arrival curves were obtained under various gas-source and ion-source operating conditions and the results printed out directly on the x-y recorder from the multichannel analyzer storage. From the graphs, either the most probable arrival time or time-to-half maximum were recorded, in arbitrary units, together with the time-of-arrival curve width at half maximum. These parameters, together with source conditions and observations, are recorded for typical tests in Table VI. To illustrate, the plots from which the first four entries of Table VI are taken are shown in Figure 10 and the plots for acetone species are shown in Figures 11 and 12. The first four curves are from a supersonic beam of N_2, and, like all high intensity beam results, show little shift with ion source conditions. The next eight curves represent parent versus fragment ion behavior from a near-effusive beam of acetone.

TABLE IV

EFFECT OF IONIZING ELECTRON ENERGY (APPARENT) AND EMISSION CURRENT ON THE SHAPE OF TIME-OF-ARRIVAL CURVES FOR A NEUTRAL BEAM ORIGINATING FROM THE EXPANSION OF 1 ATM GAS THROUGH A 0.004 IN. ORIFICE PLACED 16 IN. FROM THE ION SOURCE ELECTRON BEAM. SKIMMER DIAMETER 0.050 IN.

	Electron Energy (eV)	Emission Current (mA)	Time-of-Arrival Peak Half Width (μsec.)
N_2	50.0	2.0	139
	50.0	2.0	137
	20.0	2.0	134
	17.7	2.0	137
	16.0	2.0	137
	50.0	2.0	137
Ar	50.0	2.0	114
	50.0	1.0	114
	50.0	0.5	116

TABLE V

EFFECT OF ION INTENSITY ON TIME-OF-ARRIVAL CURVES FOR A SUPERSONIC ARGON BEAM UNDER THE CONDITIONS STATED FOR FIGURE 8

40^+ Average Count Rate (counts/sec)	40^+ Peak Count Rate (counts/sec)	Half Width of Time-of-Arrival Curve (μsec)
1,620,000	9.5×10^5	Too distorted to be meaningful
600,000	1.6×10^6	144
220,000	9.4×10^5	124
59,000	3.7×10^5	116
23,500	1.8×10^5	116
10,600	8.3×10^4	112
950	2.9×10^3	112
	Calculated half width	112

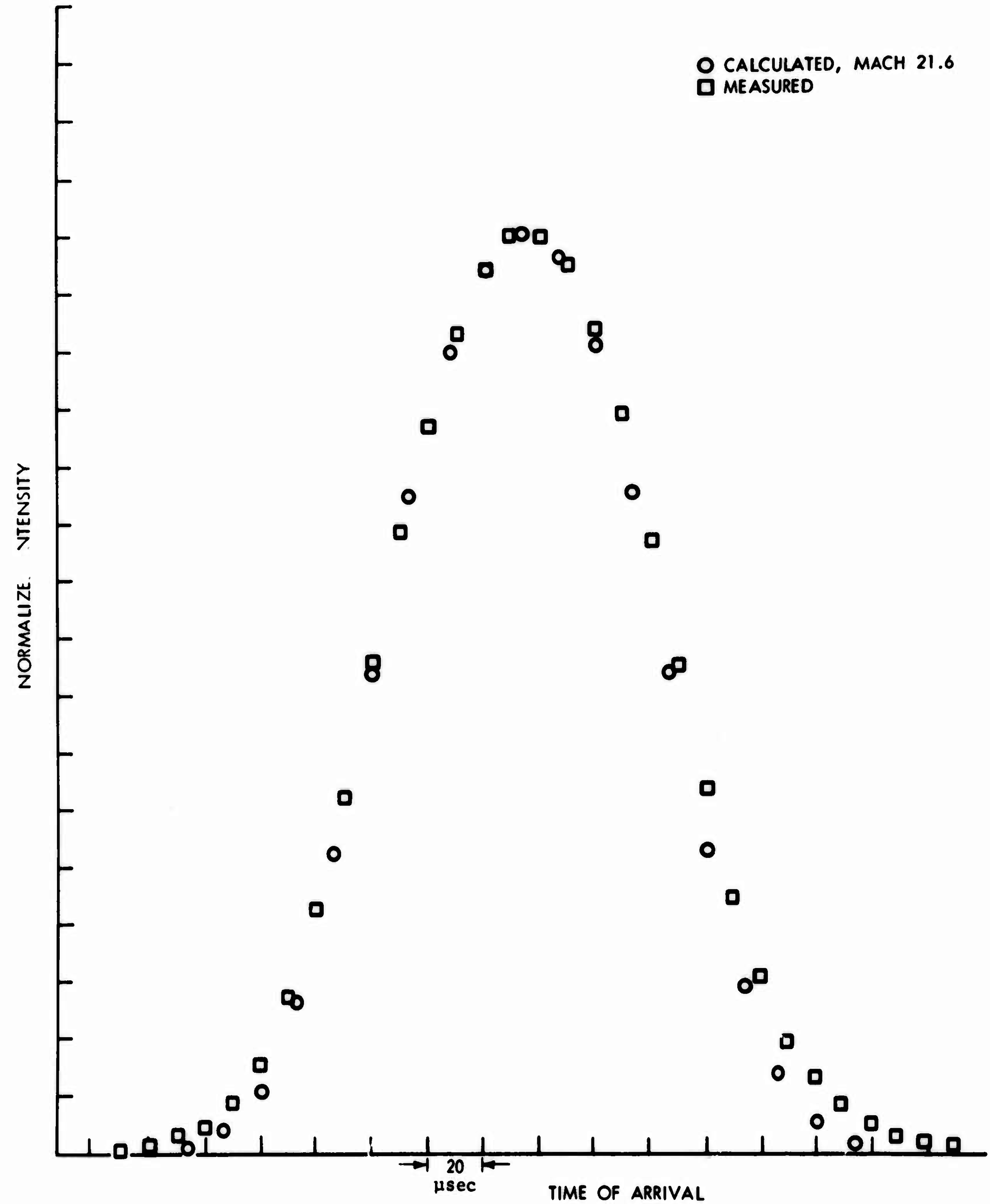

Figure 8 - Comparison of Predicted and Measured Times-of-Arrival for a Supersonic Argon Beam at a Presumed Terminal Mach Number of 21.6. Argon at 300°K, 0.1 Atm. Orifice diameter 0.040 in. Curves shifted to match at peak intensity. Electron energy 50 eV, emission current 2 mA. Ion Source No. 2.

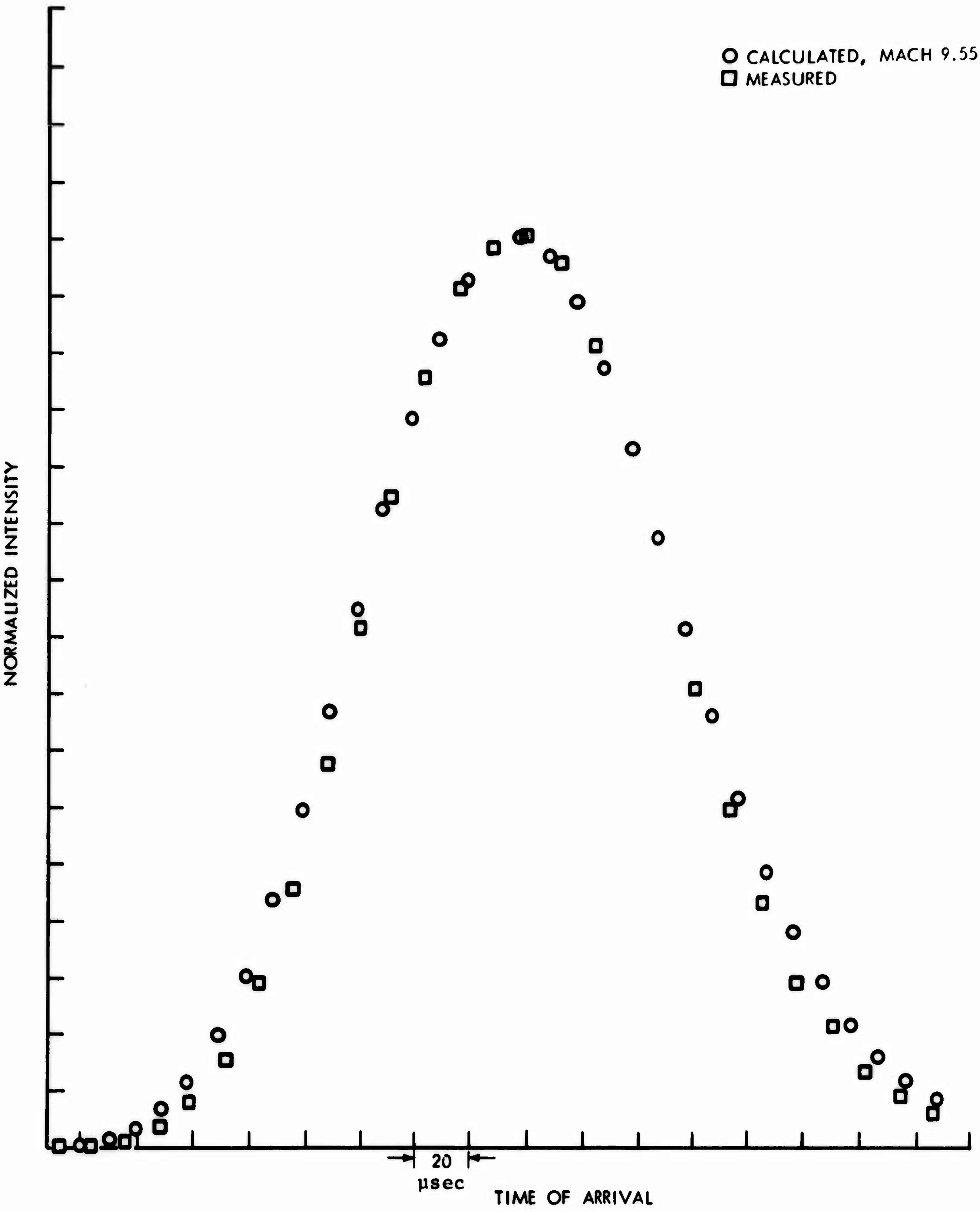

Figure 9 - Comparison of Predicted and Measured Times-of-Arrival for a Nitrogen Beam at a Presumed Terminal Mach Number of 9.55. Nitrogen at 300°K, 0.1 Atm. Orifice diameter 0.040 in. Curves shifted to match at peak intensity. Electron energy 50 eV, emission current 2 mA. Ion Source No. 2.

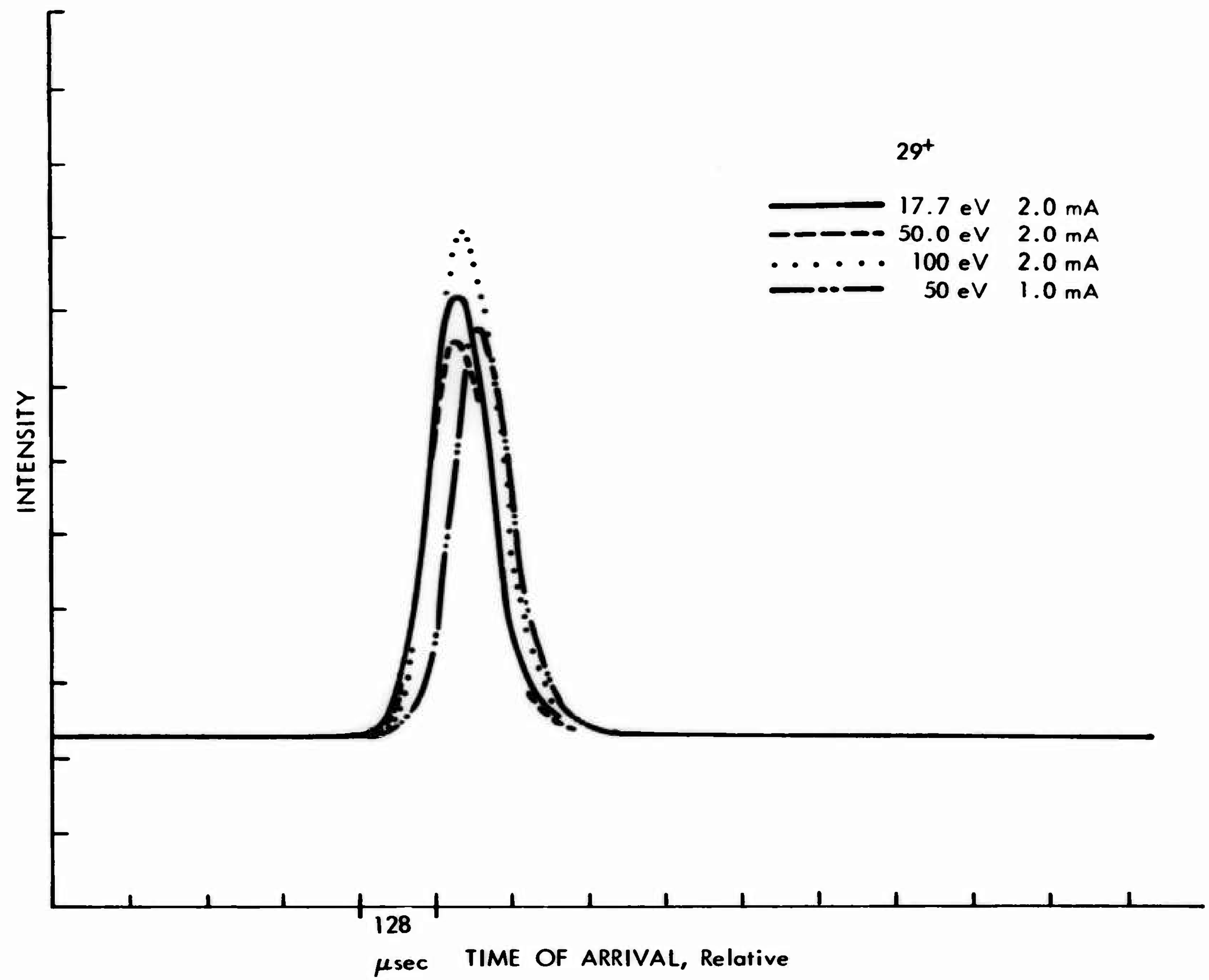

Figure 10 - Apparent Time-of-Arrival Behavior for Nitrogen From a 0.1 Atm Beam. Orifice diameter 0.040 in. Room temperature. Relative heights of curves have no significance. Ion Source No. 2.

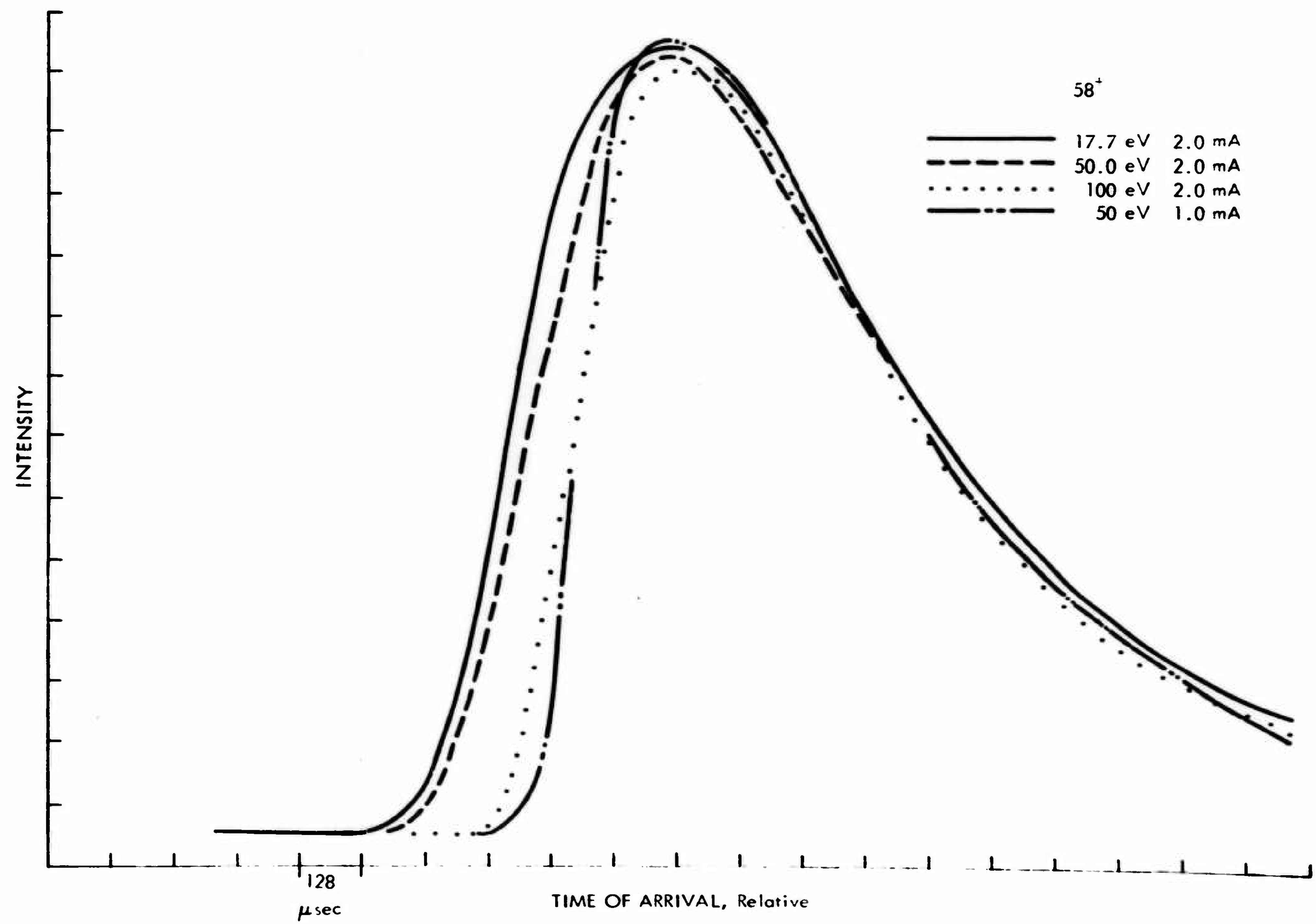

Figure 11 - Apparent Time-of-Arrival Behavior for Acetone From a Near-Effusive Beam. Orifice diameter 0.040 in. Room temperature. 58^+. Ion Source No. 2.

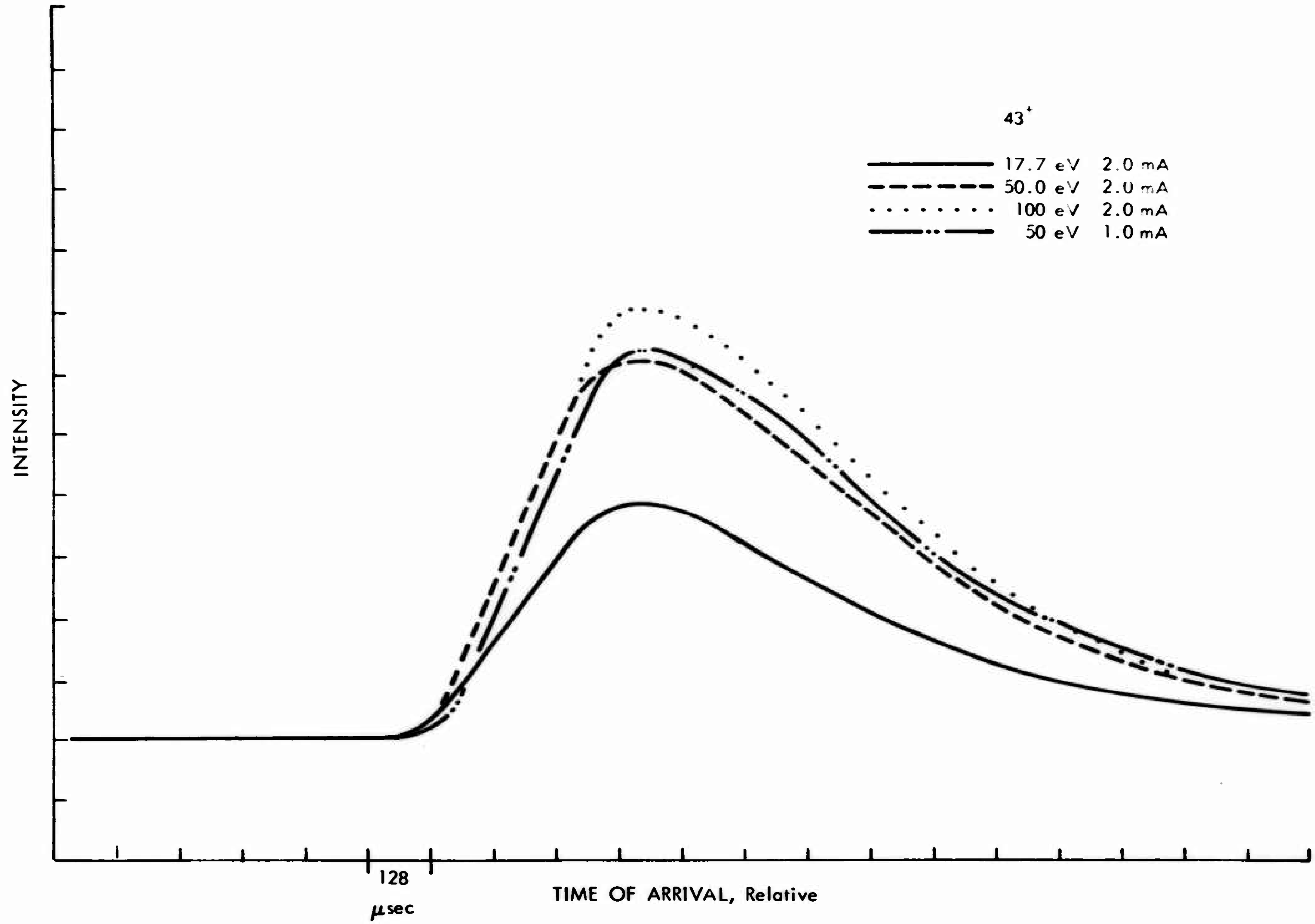

Figure 12 - Apparent Time-of-Arrival Behavior for Acetone From a Near-Effusive Beam. Orifice diameter 0.040 in. Room temperature. 43^+. Ion Source No. 2.

Shown clearly are the time delay effects with these beams as well as the marked differences in behavior of fragment versus parent ions.

Because of the possibility that clusters were present under some beam conditions, giving contributions to the peaks usually attributed to monomer, a whole series of beam formation conditions were studied partly under Office of Saline Water support. These include the heating of water vapor in a double-cell to insure large unsaturation and the absence of significant cluster concentrations. Table VI shows a representative sampling of such tests. The overall conclusion from this series was that the modified Nuclide ion-source (Source No. 2), while free of background modulation effects, exhibited an unpredictable time response that made time-of-flight measurements, on weak beams at least, unreliable and misleading. It is interesting to note that the original ion source showed the best time response at low emission currents (0.2 mA or less) while the modified source behaved best at high emission current (2.0 mA).

An effort was made to improve the time response of ion source No. 2 by raising background pressure levels substantially. When Xenon was leaked into the source region to raise the pressure (as read by the ion pump) to about 1 x 10^{-6} torr (from the 1 x 10^{-7} torr or less when only an intense supersonic beam of N_2 is present) no beneficial results were obtained. Kauffman (Ref. 13) has reported pronounced ion source pressure effects on ion trapping. so that the above result was disappointing.

c. Seeing no obvious solution to the time-response difficulties with the original modified ion source (Source No. 2) we tested another design of ion source, supplied by Nuclide (Source No. 3) which uses an electron beam defining slit between the filament and the source defining slit. At an emission current of 2 mA or less this ion source showed no evidence of ion source trapping either with high and low pressure test gases or with carbon species. However, as stated above, overall ionization efficiency was down a factor of 20 compared to Source No. 2 at the same emission current. This source could be operated at 20 mA emission, giving the same trap current and ionization efficiency as the modified original source at 2 mA, but over the single 2-hr test conducted, filament current was changing markedly and filament life is uncertain. Unfortunately, time did not permit our measuring the time response of the two-aperture source at 20 mA emission.

The previous discussion of time response behavior of the several ion sources has been considerably belabored partly to warn the unsuspecting as to the strange behavior that may be encountered in the relatively new field of time-of-arrival velocity analysis using conventional mass spectrometers. To summarize, the behavior, advantages and disadvantages of the three sources tested in most detail are listed in Table VII.

TABLE VI

BEHAVIOR OF TIME-OF-ARRIVAL CURVES FOR VARIOUS SPECIES AS A FUNCTION OF ION SOURCE PARAMETERS

Beam Gas and Conditions of Expansion	Ion	Emission Current (mA)	Electron Energy (electron volts)	Other Conditions	Time to Peak (Arbitrary Units to be Compared Only Within Each subgroup (μsec)	Width at half Max. (μsec)	Other observations
N_2, 1/10th atm, 0.040 in. diameter orifice	29^+	2.0	17.7	(Zero repeller voltage and other source	x	122	Symmetrical
		2.0	50.0	parameters peaked,	x	128	peak
		2.0	100.0	unless otherwise noted)	x + 13	122	shapes
		1.0	50.0		x + 38	122	
	29^+	2.0	50.0	Repeller	x	128	
		2.0	50.0	+ 4 V	x + 13	128	
		2.0	50.0	+ 8 V	x + 13	128	
		2.0	50.0	- 4 V	x	128	
Beam shuttered to 1/100 its full value	28^+	2.0	17.7		x	115	
		2.0	50.0		x - 13	115	
		2.0	100.0		x + 6	122	
Full Beam Again	56^+	2.0	50.0		x + 6	109	
1 Atm N_2 through water 0.005 in. diameter orifice	18^+	2.0	50.0		x	134	
	19^+	2.0	50.0		x + 6	115	
	29^+	2.0	50.0		x + 6	122	
	19^+	2.0	100.0		x + 6	115	
		1.0	50.0		x + 6	115	
		0.5	50.0		x + 6	122	
	18^+	2.0	17.7		x	128	
		2.0	100.0		x + 13	128	
		1.0	50.0		x + 19	128	
1 Atm Argon, 0.005 in. diameter orifice	18^+	2.0	50.0		x	109	
	36^+	2.0	50.0		x	101	
	80^+	2.0	50.0		x + 13	109	
		2.0	100.0		x + 13	101	

TABLE VI (Concluded)

Beam Gas and Conditions of Expansion	Ion	Emission Current (mA)	Electron Energy (electron volts)	Other Conditions	Time to Reach Half Intensity, Relative Times in μsec	Width at Half Max. (μsec)	Other Observations
Acetone, 0.040 in. orifice, room temperature	57^+	2.0	17.7		x	231	Symmetrical with slow tail
		2.0	50.0		x + 19	218	
	43^+	2.0	17.7		x	198	
		2.0	50.0		x + 6	218	
		2.0	100.0		x + 6	205	
		1.0	50.0		x + 13	205	
	58^+	2.0	17.7		x + 6	198	
		2.0	50.0		x + 26	198	
		2.0	100.0		x + 26 and x + 179	320	Two peaks
		1.0	50.0		x and x + 282	473	Two peaks
Icebath and throttling to reduce acetone beam strength by factor of 20	43^+	2.0	17.7		x	768	
		2.0	50.0		x	832	
		2.0	100.0		x + 26	819	
		1.0	50.0		x + 32	807	
		0.5	50.0		x + 6	819	
	43^+	2.0	50.0		x	876	
		2.0	50.0	J2 Full CCW	x	890	
		2.0	50.0	J2 Full CW	x	857	
		2.0	50.0	Repeller + 9.5	x + 13	870	
		2.0	50.0	Repeller - 5.0	x - 13	845	
	15^+	2.0	50.0		x	820	
		2.0	100.0		x - 19	864	
	58^+	2.0	17.7		x - 13	884	
		2.0	50.0		x + 32	851	
		2.0	60.0		x + 32	851	
		2.0	70.0		x + 51	832	
		2.0	80.0		x + 64	819	
		2.0	90.0		x + 96	787	
		2.0	100.0		x + 122	749	
		1.0	50.0		x + 128	717	
		0.5	50.0		x + 198	761	
		2.0	50.0	Repeller + 5	x + 83	819	
		2.0	50.0	Repeller - 4	x - 19	870	
Beam attenuated another factor of 10 by lowering source pressure	43^+	2.0	50.0		x	985	
		2.0	100.0		x + 19	935	
	58^+	2.0	50.0		x + 32	896	
		2.0	100.0		x + 128	768	

TABLE VII

COMPARISON OF TIME RESPONSE OF DIFFERENT ION SOURCES

Source Identification	Pertinent Features	Relative Sensitivity	Time Response and Behavior
Original Source (Source No. 1)	Single electron beam entrance slit 0.025 in. x 3/16 in.	(at 2.0 mA, 50 eV) 100	Very poor at > 0.2 mA emission. Sometimes worse at low voltage. Sensitive to repeller voltage. Not tested with weak beams or fragment ions.
Modified Original Source (Source No. 2)	Single electron beam entrance aperture of 1/32 in. dia	12	Good at 2 mA, 17 eV for strong beams. Worse the higher the voltage, lower the emission, weaker the beam. Not tested above 2.0 mA. Worse with parent ions than fragment.
Nuclide Dual-Aperture Source (Source No. 3)	Two slits for electron beam: 0.062 in. aperture and 0.040 in. x 0.250 in. slit	0.6	Good time response for strong and weak beams, parent and fragments at 100 eV or less, 2 mA or less. Not tested at > 2.0 mA.

At the moment we appear to have to give up sensitivity in order to get faithful time response. Presumably there exists one ion source configuration which more nearly optimizes both sensitivity and time response, but we do not plan further extensive experimentation. At this point we will need to use ion Source No. 2 for maximum sensitivity to large clusters and Source No. 3 for quantitative use of TOF analysis of fragmentation, measurement of temperature, and detection of the onset of continuum flow. Source No. 1 is ruled out because of extensive modulation of signals from background gas.

5. Rapid peak switching. Because of the rapid deterioration of carbon cells in vacuum at temperatures beyond 3000°K, we are planning to acquire data in as short a time as possible. In the case of making time-of-arrival velocity measurements, the use of ion counting seems most advantageous and the multichannel analysis scheme used has been described. For the central task of measuring carbon species ratios as a function of temperature, whether from equilibrium or freely evaporating surfaces, the following considerations apply. In reaching the desired temperature and pressures (approaching 1 atm) we will likely be forced to carry out short heating excursions to the highest temperature, gathering species ratio or TOF data during the short times before the cell fails or evaporated carbon interferes. Since it may be difficult to obtain reproducible heating excursions and periods of constant temperature, and since cell geometry may change during heating, much more reliable data can be realized by always measuring ratios of two species during each heating. Consequently, we have built a simple peak switching device which allows us to dwell alternately on each of two peaks for periods as short as 10 msec.

The peak switching is accomplished by the direct process of switching between two independent high voltage power supplies for the ion source voltages. A schematic of the system is shown in Figure 13. The switch is a vacuum relay manufactured by Torr Laboratories and having a claimed switching time of 4 msec make and 4 msec break. The second power supply is a Fluke, Model 415B, ultimately to be replaced by a 0 to 5,000 V supply of similar stability. When ion-counting is used, circuitry is included to disable the counting system during the few milliseconds of actual voltage excursion during switching. Presently the switch is controlled either manually or by an Atec counter-timer which can conveniently operate at switching periods of from 1/10 to 10 sec. Each time the voltage is switched, the multichannel analyzer is advanced one channel. While in a given channel, the analyzer operates as a reversible counter with reversal synchronized with the molecular beam chopper (see Figure 1). In this manner a record of phase-locked signal at any two chosen charge/mass ratios can be obtained. With 10 sec/channel, the 1024 channels permit a digital record of a heating history lasting some 170 min. Rapid heatings of 1.7-min duration could be fully recorded with a 1/10-sec dwell time on each of two peaks.

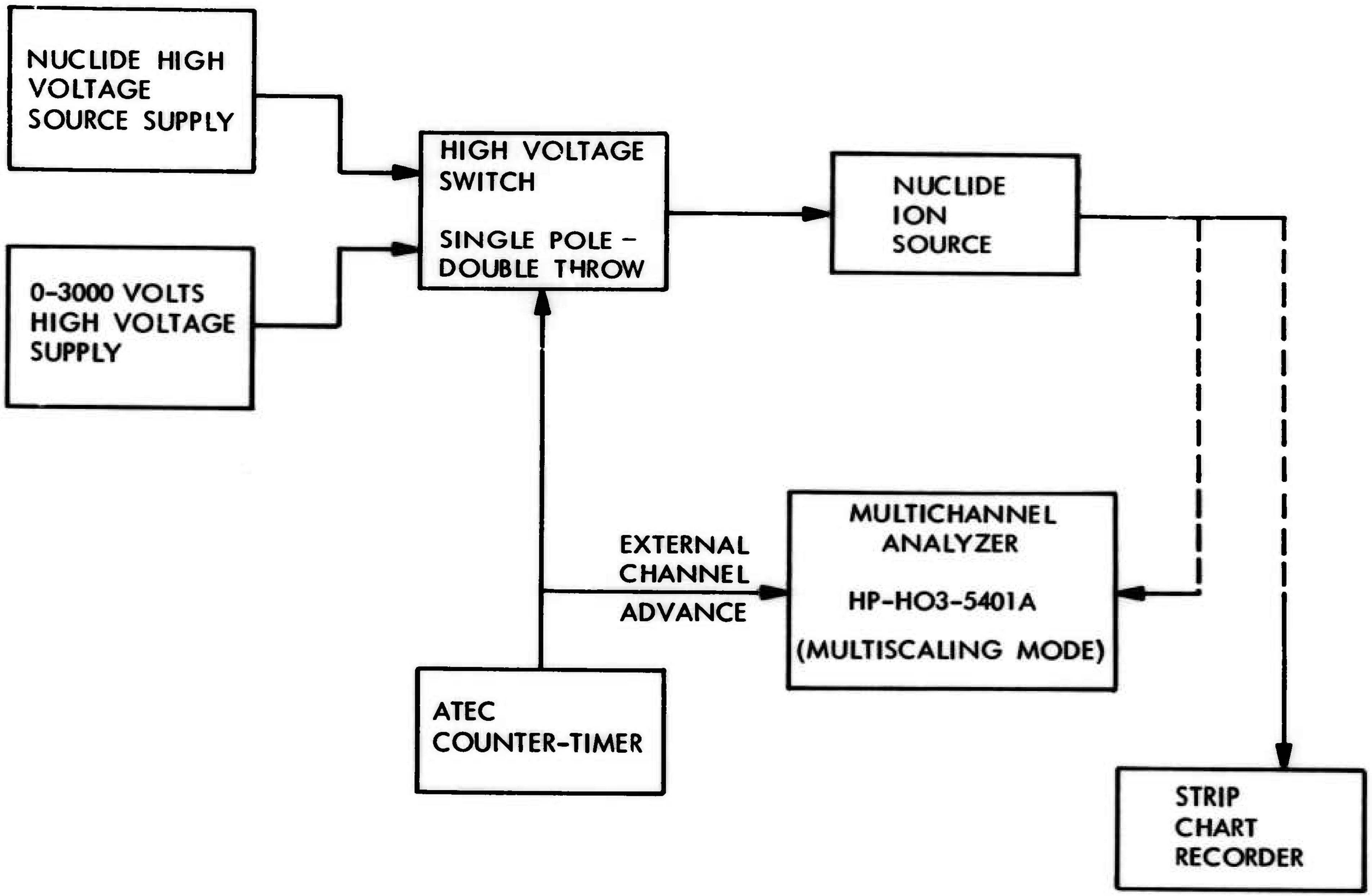

Figure 13 - Schematic of Rapid Peak Switching Method in Use With Either Analog Detection or Ion Counting

The peak switching system works very well in practice. Switching times of a few milliseconds are realized and there is no evidence of major noise problems or ringing as a result of the rapid voltage change. Figure 14 shows a multichannel analyzer record of switching between 28^+ background peak and zero voltage.

The advantages of using ion counting and digital storage in following carbon species ratios over a big temperature range are great. First, with a storage capacity of 10^6 counts/channel, the multichannel analyzer can cover a large range of intensities for a given species and can simultaneously measure two species differing widely in intensity. By dwelling 100 times longer on the weak peak, for example, one could expect to detect phase-locked signals from peaks at the 1 ppm level of C_3^+ for example. Second, the digital data are stored without the necessity of choosing a time constant, as is required in analog detection. On subsequent analysis of the data, the peak signals can be averaged over any desired number of alternate channels to smooth out noise.

Unfortunately, our first attempts to use ion-detection and peak-switching on carbon vapor species resulted in failure due to RF noise interference. Two factors appear responsible. First, the multiplier gain at the time RF noise-free counting conditions were first established, was about 1×10^6 at the chosen dynode string current. This gain has deteriorated over the course of ion source testing to a value of about 2×10^5 as previously described. Although slightly higher multiplier gains can be used, the system is presently marginal with respect to RF interference discrimination. The second factor complicating the use of ion counting with electrostatic peak switching is that of reduced gain at the lower voltages used for the higher mass ion. In a counting situation where one is barely discriminating between ion pulses and noise, this change of gain can lead to quite different fractions of the two ions being counted and would require calibrations and stability of discrimination levels.

It appears that we will have to take one or more of the following steps to implement the ion-counting, peak-switching scheme for carbon vaporization characterization: (1) increase multiplier gain by replacement, cleaning or reactivation of multiplier elements; (2) reduce RF interference by more complete shielding of the generator, leads and work coil; and (3) reduce noise pickup in the counting system.

The peak switcher works well using the phase-locked amplifier and analog, strip-chart detection. With a 1/10-sec time constant on the phase-locked amplifier and about 10-sec intervals on each peak, records such as are shown in Figure 15 can be obtained. Figure 15(a) shows 36^+ versus 24^+ during a short heating. Note that both peaks are phase-locked. Figure 15(b) shows 36^+ versus a background peak, 26^+, that might have shown contributions from

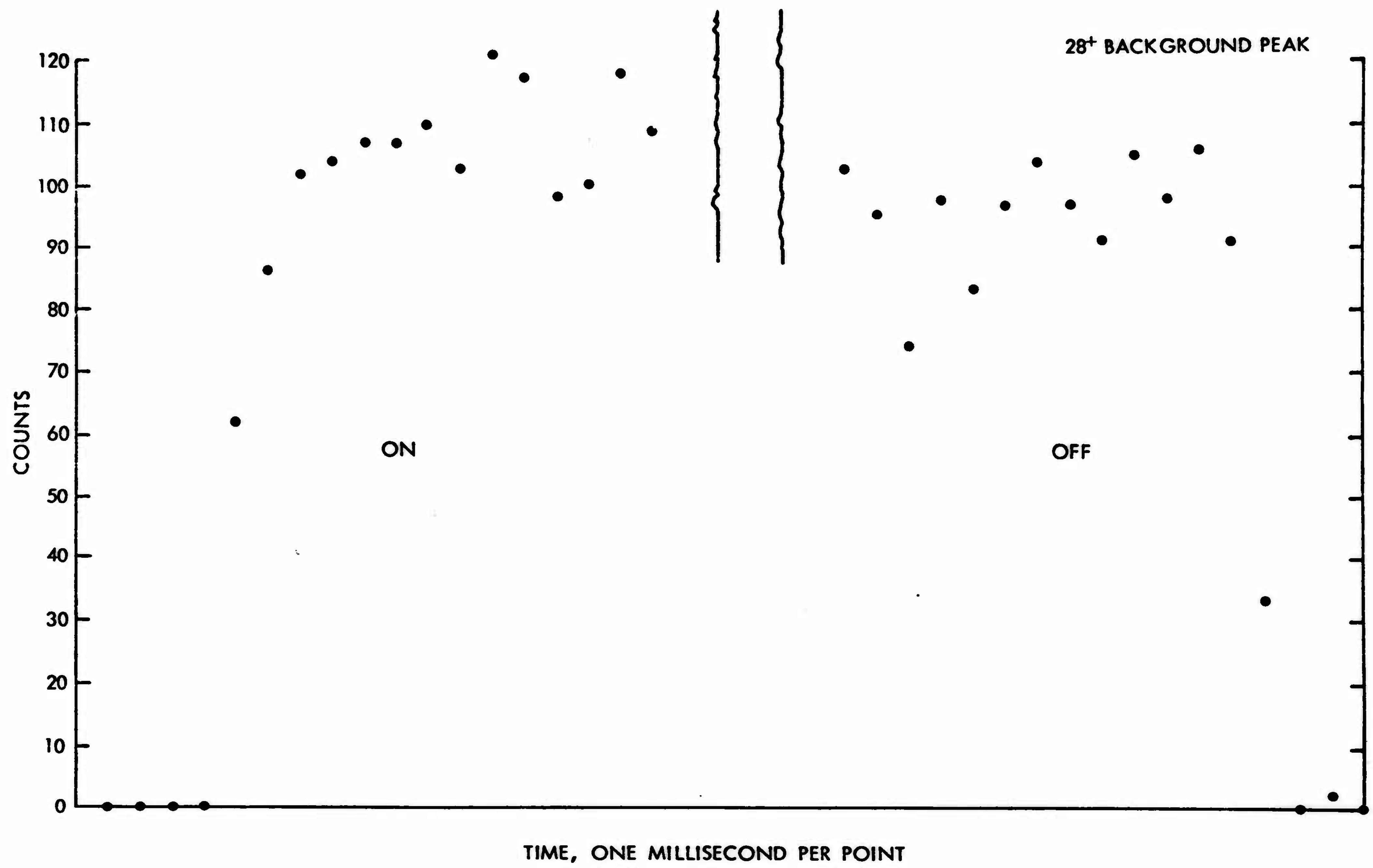

Figure 14 - Multichannel Analyzer Record of Behavior of Peak Switcher. Shown is the switching from zero voltage to 28^+ background peak.

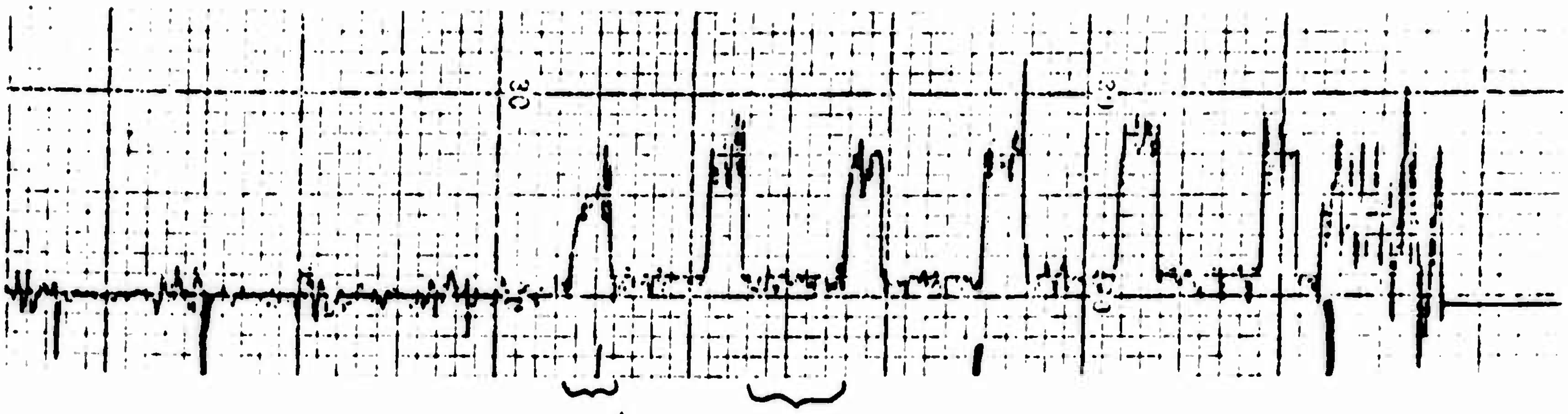

15(a)

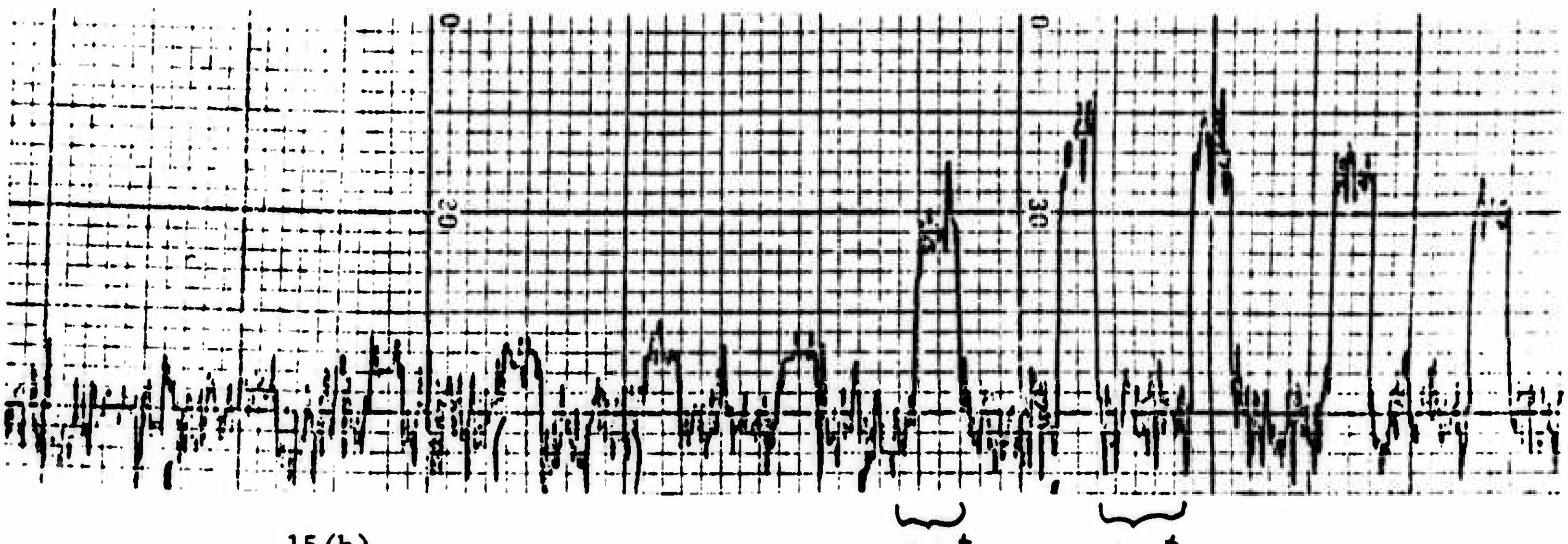

15(b)

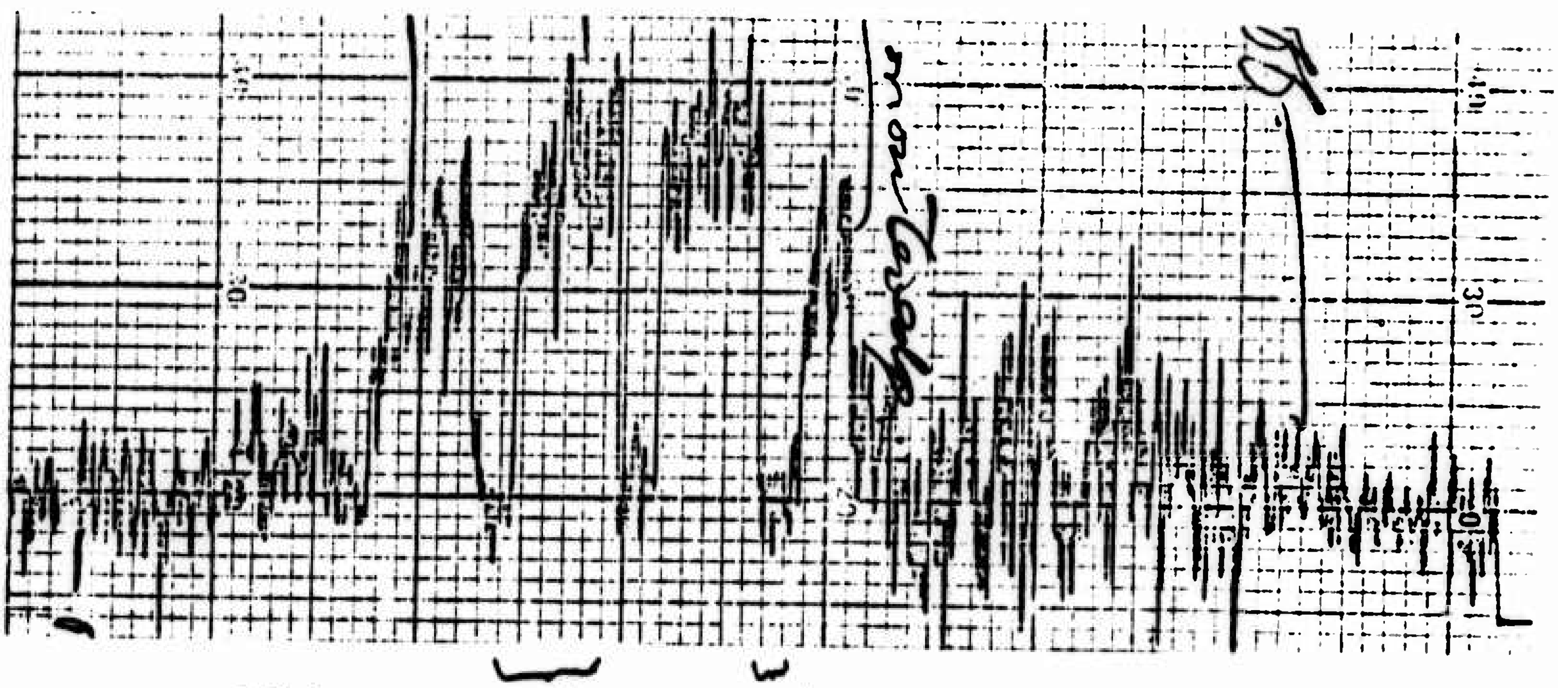

15(c)

Figure 15 - Strip Chart Records of Phase-Locked Amplifier Output When Peak Switcher is in Operation During Short Carbon Heatings. The carbon vapor beam is chopped at 300 cycles/sec. Chart speed is 20 sec/in (major chart division).

$C_2H_2^+$ from outgassing. The two peaks being monitored in Figure 15(c) are 37^+ ($C^{12}C^{12}C^{13+}$) (about 3% of the 36^+ peak) and 60^+ (C_5^+). The carbon vapor source and temperature were poorly defined during these test heatings. The strip chart shows C_5^+ to be less than 1% of the C_3^+ intensity. At higher pressures, the analog scheme should be useful in following C_3^+/C_n^+ ratios, if the appropriate C_3^+ isotopic peak is used to roughly approximate the intensity of the C_n^+ chosen for the study.

C. Carbon Heating and Vapor Source

A major part of the present research has been to develop a source of equilibrium carbon vapor at temperatures substantially beyond the previous limit of about 3200°K. Of the various vaporization schemes originally considered (Ref. 1) we have chosen to concentrate solely on RF heating of self-contained, pyrolytic graphite shielded, Knudsen cells as discussed in Ref. 2, p. 26. The present status of cell design and heating arrangements will now be reviewed.

1. Cell design. In the Second Annual Progress Report (Ref. 2) heating results with a single-walled, partially slotted Knudsen cell were presented and what was hoped to be an improved version (Ref. 2, Figure 13) was described. This double-walled cell was test heated using a 1-7/8 in. I.D. four-turn work coil and a step-down RF transformer.

Several observations are worth noting. It was conceived that the open slots could be replaced by a series of 1/32 in. dia holes drilled lengthwise through the outer shield walls, at staggered positions around the circumference and at overlapping diameters. In this way, each complete shell of the PG wall would be interrupted at some point, and in view of the very large transverse electrical resistance, little current would be induced in the shield by the RF.

The first RF heating test, without the inner susceptor, unfortunately showed efficient heating of the shield. In fact it was necessary to slot the shield rather deeply and at more than one point, in order to achieve major heating in inner, unslotted susceptors. Furthermore, the 3/16-in. thick shield walls suffered severe delamination so that their shielding varied with time. In tests with this cell, which contained 1/8-in. thick lids, this delamination caused the upper lid to come loose, allowing excessive escape of radiant energy and carbon vapor from the interior. Quite satisfactory temperature differences were observed between inner and outer surfaces, however. With inner black-body temperatures (uncorrected) of about 2500°C, the end-lid surface temperatures were about 1700°C with the narrow slots indicating temperatures of 2150°C. The cylinder outside walls were about 1500°C with slot temperatures of 2100°C. These temperature differences should be sufficient to permit the desired inner temperature with tolerable losses of heat

and vapor from the outside of the cell. There were still hot spots where the lids fit the cylinder walls, and these hot areas were enlarged in the test heating due to the lids partially loosening from the cylinder.

As an economy move, while other aspects of heating were being studied, we used a fully slotted outer PG shield with slotted PG end lids and unslotted inserts of ATJ graphite either as thin-walled susceptors or with solid cylinders for "free" evaporation work. Results and problems encountered with such cells are discussed in the following section.

2. RF heating. In Ref. 2, p. 19, early problems with arcing and discharges were discussed for systems using either direct heating of the cells with the work coil in the vacuum system or using the current concentrator with the work coil outside the vacuum. The use of an RF transformer alone was not sufficient to prevent arcs, at least with the combination of coupling, coil and cell geometry that we tested. We recently learned from Dr. Ed Storms and Mr. Don Hall, at Los Alamos (Ref. 15), that they have successfully heated small objects to about 4000°K in vacuum, using current concentrators inside pyrex tubes, with the work coil on the outside. No arcing was observed until sufficient carbon had built up to bridge the slot in the current concentrator. It thus appeared profitable to return to the current concentrator approach, which was unsuccessfully tried initially, taking care this time to adequately shield the pyrex walls and to provide improved pumping around the concentrator. The overall heat load to the concentrator was expected to be manageable due to the excellent gradients achieved across even single-walled PG Knudsen cells.

Before going back to the current concentrator used early in the program, a few final tests were made with the work coil inside the vacuum system both with and without the current concentrator. With the small work coil and step-down transformer used in the last carbon vaporization work, another heating was tried in which the graphite Knudsen cell and shields were electrically isolated from ground. The usual arcing limitations were present, however, so the current concentrator and a large work coil were placed inside the vacuum chamber. With the step-down transformer, coupling to the large work coil was too poor to permit adequate heating. Without the step-down transformer, arcs occurred around the RF vacuum feedthrough as had earlier been noted. We then abandoned completely the use of the vacuum RF feedthrough and the work coil inside the vacuum and returned to the current concentrator as depicted in Figure 7 of Ref. 2.

Two major changes were made in the old current concentrator setup to improve its performance and to help diagnose the cause of limitations due to arcing or discharges. First, an ion gauge was installed at the dead end viewing port just below the lower flange to monitor the buildup of pressure in the vicinity of the bottom of the Knudsen cell. Second, the large diaeter copper cylinder of the current concentrator was extended over the full

length of the Pyrex pipe to completely shield the pyrex from direct radiation from the hot graphite. The small diameter segment of the current concentrator was placed in the middle of the large section, not offset as shown in Figure 7 of Ref. 2.

A five-turn work coil about 5-1/2 in. dia was placed on the outside of the 4-in. I.D. Pyrex pipe. The upper and lower flanges were water-cooled as was the current concentrator. The bottom two flanges, which are in metal contact with the stainless steel water pipes that support and cool the current concentrator, were initially isolated from ground by 3 ft. of braided rubber hosing although this appeared to make no difference and direct connection of copper lines is now used.

After correcting some troublesome leaks in the water cooling pipe welds, the system was tested with a variety of cell and shield configurations. The results were encouraging. In no cases did destructive arcs or discharges occur inside the vacuum system. In one case the Knudsen cell tipped over against the side of the current concentrator causing visible arcs and a purple glow, but even then the RF generator did not trip off although large pressure surges accompanied the arcing.

The most successful heatings to date used the cell and shield configuration shown in Figure 16. The legs are "UCAR" AGSR graphite, the pins are made from vitreous graphite 1/8-in. rod, the lids are slotted 1/8-in. thick pyrolytic graphite plate, the outer shield is fully slotted 1 in. O.D. by about 1/16-in. wall pyrolytic graphite tubing and the inner susceptors range from solid ATJ or PG cylinders (for free surface evaporation studies) to ATJ graphite two-piece cups for Knudsen studies.

With an ATJ thin-walled cylinder as susceptor and containing a baffle, orifice temperatures of 3500°K have been reached. (Some uncertainty exists due to the large window correction involved.) With the inverted ATJ cups shown in Figure 16, temperatures up to 3360°K have been measured through the offset orifices. Achievement of these temperatures consitutes an important breakthrough for this program, as we are now in a position to observe near-equilibrium vapor composition at temperatures well beyond the previous high of 3200°K, reported for C_3 only, by Steele (Ref. 5).

No physical evidence of arcing between cell and concentrator was seen. The chief problems encountered were: (1) Pressures rose to values in the 1×10^{-3} torr range in the bottom half of the current concentrator, due to the limited pumping speed around the Knudsen cell and between the Pyrex and current concentrator. (2) Windows rapidly coated with carbon vapor (and particles, when ATJ inserts were used) making temperature measurements uncertain after a few minutes of heating at the higher temperatures. In addition, flakes of graphite peeled off the inner sides of the large diameter

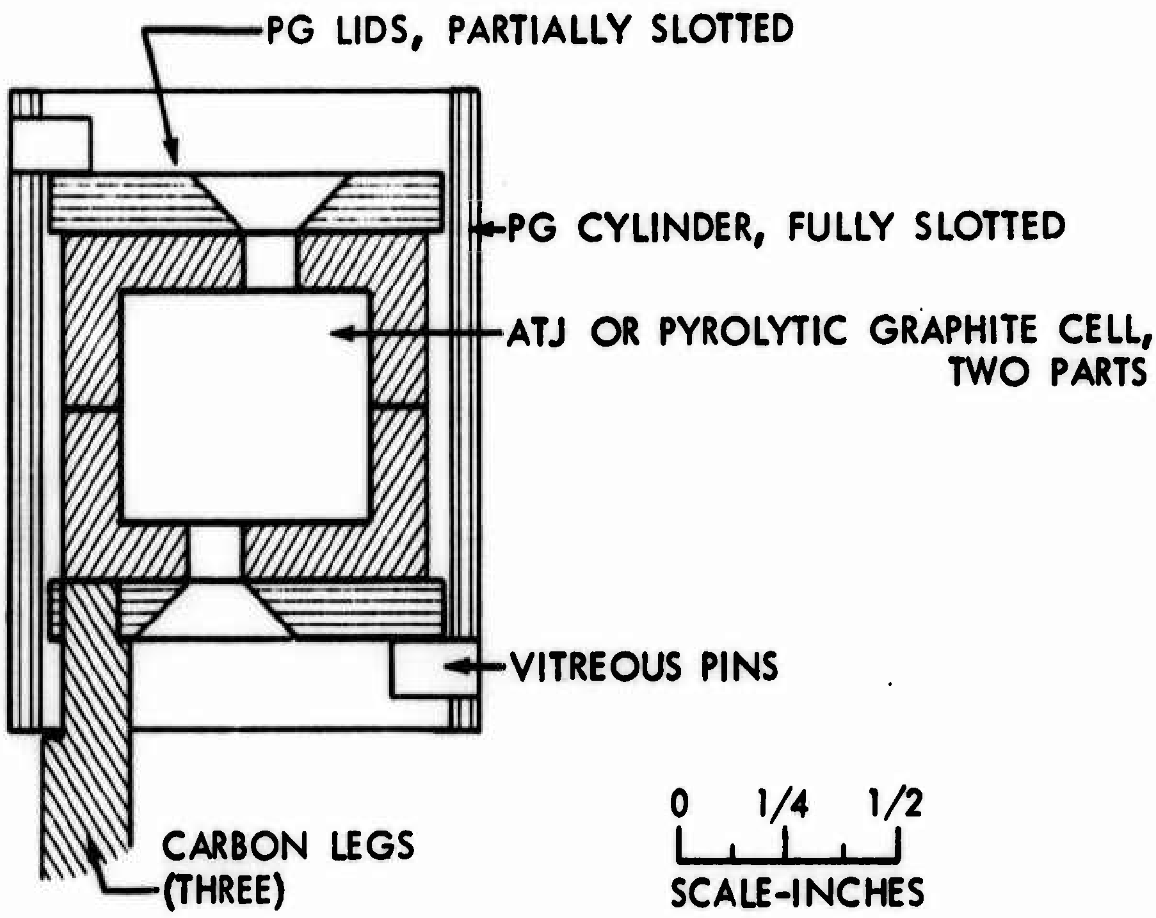

Figure 16 - Knudsen Cell and Shield Configuration Used in the Most Successful Induction Heating to Date

section of the current concentrator after several heatings and coolings, causing obstruction of the lower viewport and occasional arcs when the flakes bridge the cell-concentrator gap. Figure 17 shows an extreme case of such flaking. (3) The upper lids of the cells tended to levitate out of the concentrator, forces being sufficient in one case to toss the entire susceptor and upper lid onto the ledge of the current concentrator. (4) Excessive material loss occurred out the center of the slot in the fully slotted PG shield. The slot, on occasion, widened to 1/4 to 1/2 in. at the center and entire solid cylinders of ATJ (1/2 x 13/16 in. dia) vaporized through the enlarged slot. Figure 18 shows such widening as well as the buildup of carbon on the current concentrator directly opposite the side slot.

To overcome these problems, the following modifications have been made. (1) Considerably increased pumping is supplied to the lower half of the current concentrator by joining a 4 in. dia pipe from the bottom of the current concentrator up to a side port in Stage 1 of the beam sampling system. (2) A viewing port with a continuous strip of transparent Teflon tape which can be mechanically advanced past the viewing window, has been installed on the diagonal laser-viewport shown in Figure 11, p. 38, Ref. 1. Thus, we can now view the same orifice as the mass spectrometer; gravity prevents troublesome particulates from fouling the Teflon tape mechanism; only one orifice is needed, giving better black body conditions and allowing simplified cell design with one central leg. (3) A cell design employing 1/8 in. dia vitreous carbon pins seems to prevent levitation forces from tilting or moving the cell. (4) The problem of preventing vapor loss from the side slot of the outer PG shield requires further experimentation. We currently plan to return to the use of a single, only partially slotted PG cylinder as both susceptor and shield.

The RF heating system currently in use is shown schematically in Figure 19. Additional water cooling of the current concentrator walls and shielding of the lower Pyrex "T" section may be required later. Experience to date indicates that successful heating will be of short duration in vacuum due to the inherently large mass transport. At temperatures beyond 3200°K a mechanical drive may have to be added to the Teflon tape advance mechanism to maintain a clean window, second by second. Some photoelectric means of monitoring at least relative temperatures may well be needed for fast heating cycles, with point checks based on the disappearing filament pyrometer. The problem of light scattering and absorption by nucleated carbon vapor in the optical pyrometer path must not be forgotten.

Figure 17 - Photograph of Flakes of Carbon Covering Graphite Cell and Current Concentrator After Several Extensive Vaporizations

Figure 18 - Photograph of Inside of Current Concentrator and Carbon Cell Similar to That Shown in Figure 16 but With Solid ATJ Graphite Insert

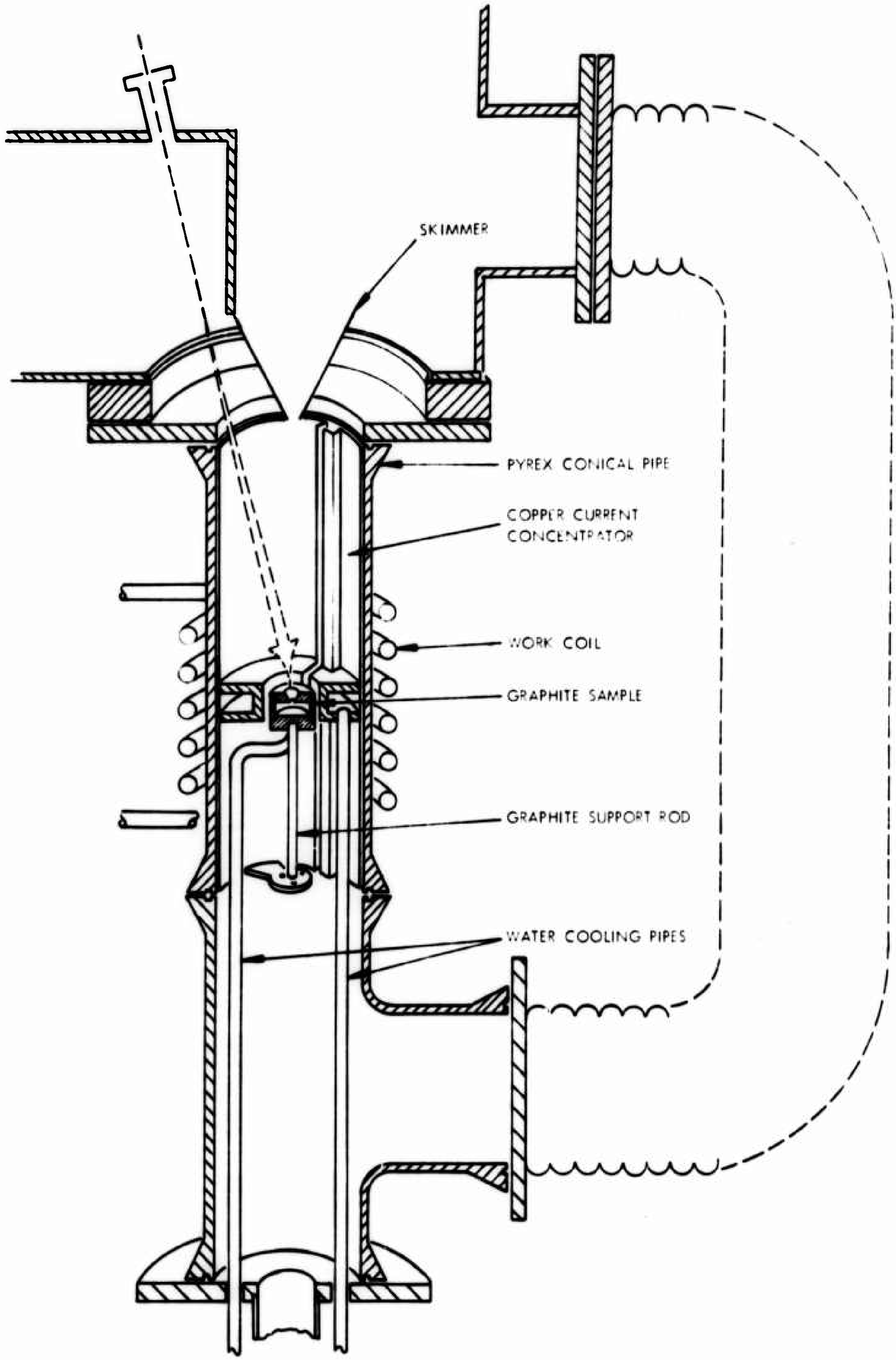

Figure 19 - Schematic of the Induction Heating Arrangement Currently in Use

D. Mass Spectra of Carbon Vapor

Early results of equilibrium vapor mass spectra, together with sensitivity estimates, have been given in Ref. 2, pp. 10 and 23. The past year's mass spectrometry has involved almost entirely the problem of the time-of-flight analysis of carbon vapor, the time response and other diagnostic work with different ion sources and the implementation of the fast peak switching with reversible ion counting. In this section we present the results obtained in TOFing carbon vapor and add a comment about new evidence as to the expectation of the onset of continuum effects in high temperature systems.

1. TOF velocity analysis of carbon species.

a. The first measurements of velocity distributions for carbon species were made with the unmodified, original Nuclide high-efficiency ion source (Source No. 1 above). Measurements were made at 0.2 mA emission current and 17.0 to 50 eV only, conditions which at the time were believed to give adequate time response based on supersonic argon beam results.

During heating tests with the Knudsen cell shown in Figure 9 of Ref. 2, time-of-flight analysis was carried out on C_1^+ and C_3^+ peaks at two electron energies. The carbon vapor was presumed to be coming mainly from the 1/16 in. dia orifice as evidenced by the observed C_1^+/C_3^+ ion ratios which agreed with literature equilibrium values, the reasonably sharp peaking of the beam with cell position (not too definitive since a 3/16 in. dia skimmer was used) and visual observation of steep temperature gradients along the outside tapered orifice surface. Pertinent parameters for the TOF experiments are shown in Table III. (The assumed source temperature of 2700°K may be 100° to 200° hotter than the actual temperature when the C_1^+ and C_3^+ data were taken but this discrepancy should not affect the qualitative observations.)

With the carbon source aligned for maximum 36^+ beam, TOA curves were readily obtained in several minutes' time at about 2600°K. No RF interference was present as such, but during these heatings there were periodic arcs which produced short bursts of "counts" and spoiled many of the multichannel scaling curve accumulations. (The shielding was behaving badly during these heatings, and this problem has not recurred.) The first noise-free TOA curve obtained for 36^+ at 50 eV ionization energy is shown in Figure 20(a). Subsequent curves for 36^+ at 50 eV, obtained over several hours of heating on two consecutive days, are shown in Figures 20(b), (c), and (d). The outstanding feature of these curves was the marked hump on the low velocity side. It was tempting to ascribe this hump to the contribution of a higher carbon cluster to C_3^+ by dissociative ionization. The decrease with time of this low velocity contribution was a complicating factor and of unknown cause.

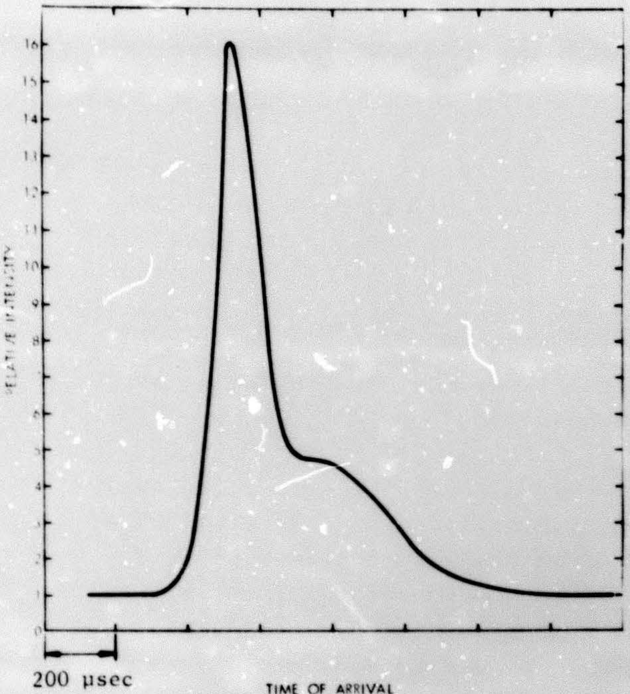

(a) Early in First Heating.
Temperature ≅ 2600°K.

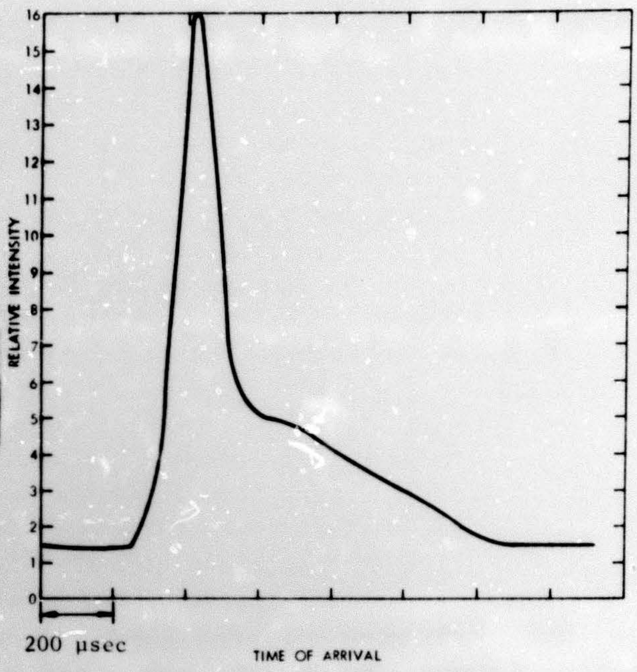

(b) Later in First Heating.
Temperature ≅ 2600°K.

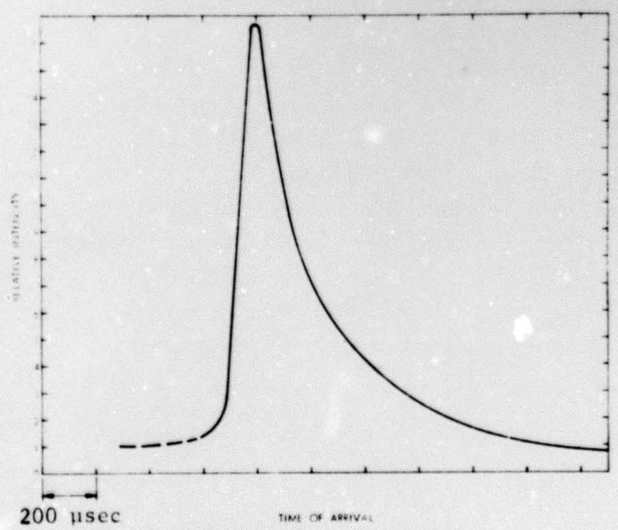

(c) Early in Second Heating.
Temperature ≅ 2450°K.

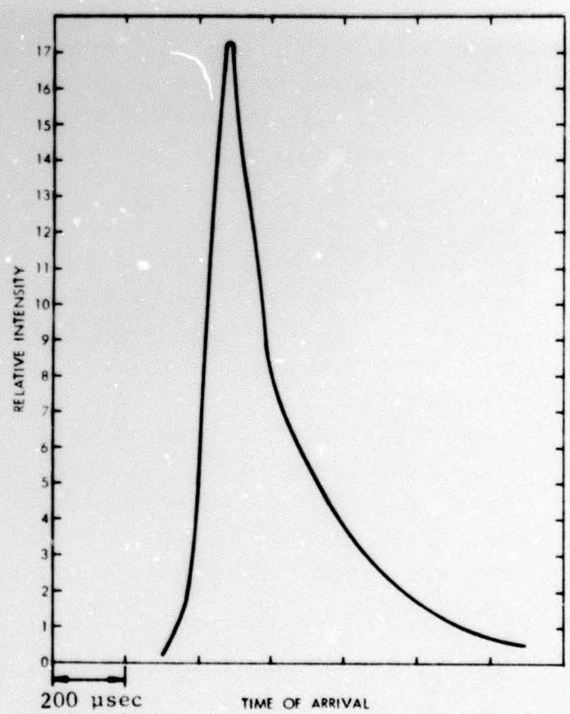

(d) Later in Second Heating.
Temperature ≅ 2700°K.

Figure 20 - Time-of-Arrival Behavior of a Chopped Beam of Carbon Vapor. 36^+ at 50 eV electron energy and 0.2 mA. Ion Source No. 1.

In preliminary diagnosis of the source of the complex C_3^+ TOA curve shape, measurements were made on C_3^+ at 17 eV. The plot of Figure 21 shows a peak-intensity normalized overlay of 36^+ at 50 eV and 17 eV showing the possible magnitude of the $C_{n>3}$ contribution, if real. Similar behavior with voltage was shown by C_1^+, as seen in Figure 22. In this case it has long been supposed that higher clusters contribute to C_1^+, at 50 eV. For both C_1^+ and C_3^+ the computed TOA curves were broader than the 17 eV curves, preventing any quantitative analysis of the broadening at 50 eV.

These results were suggestive of the value of time-of-flight analysis of observed carbon ions as carbon temperatures increase. If even 10% of the C_3^+ at 50 eV electron energy was coming from $C_{n>3}$, then this would indicate extensive fragmentation of higher clusters and an underestimate of $C_{n>3}$ from measurements at 50 eV and possibly from low voltage measurements as well.

b. By the next opportunity to TOF carbon vapor on the Nuclide, we had installed the modified ion source (Source No. 2) with its demonstrated adequate time response to supersonic beams from 17 to 50 eV and at 2.0 mA emission. A series of time-of-flight measurements were made on C_1^+, C_2^+, and C_3^+ formed from neutral vapor freely evaporating from both ATJ and PG surfaces. The results are shown in Table VIII and also, for C_3^+, in Figure 23. The behavior from 17 to 50 eV at 2 mA is similar to that observed above, but this time both higher electron energies and lower emission currents were tested with results that are seen to raise serious doubts about the ion source behavior. As discussed above, these results led us to the series of tests with gas beams and to tests with the dual aperture ion source (Source No. 3).

c. With Source No. 3 and freely evaporating graphite at about 2700°K, we repeated time-of-flight measurements on C_3^+ and observed substantially less delay and broadening from 17 to 50 eV (if any) than with the previous two ion sources, as shown in Figure 24. Although some additional measurements should and will be taken with this source that shows adequate time response under all beam conditions tested (Source No. 3) there no longer is the evidence that major contributions to C_3^+ are present from higher neutral clusters. Hence the priority shifts to using time-of-flight measurements, probably at or near 17 eV, to determine source temperature and the onset of continuum-flow perturbations of composition.

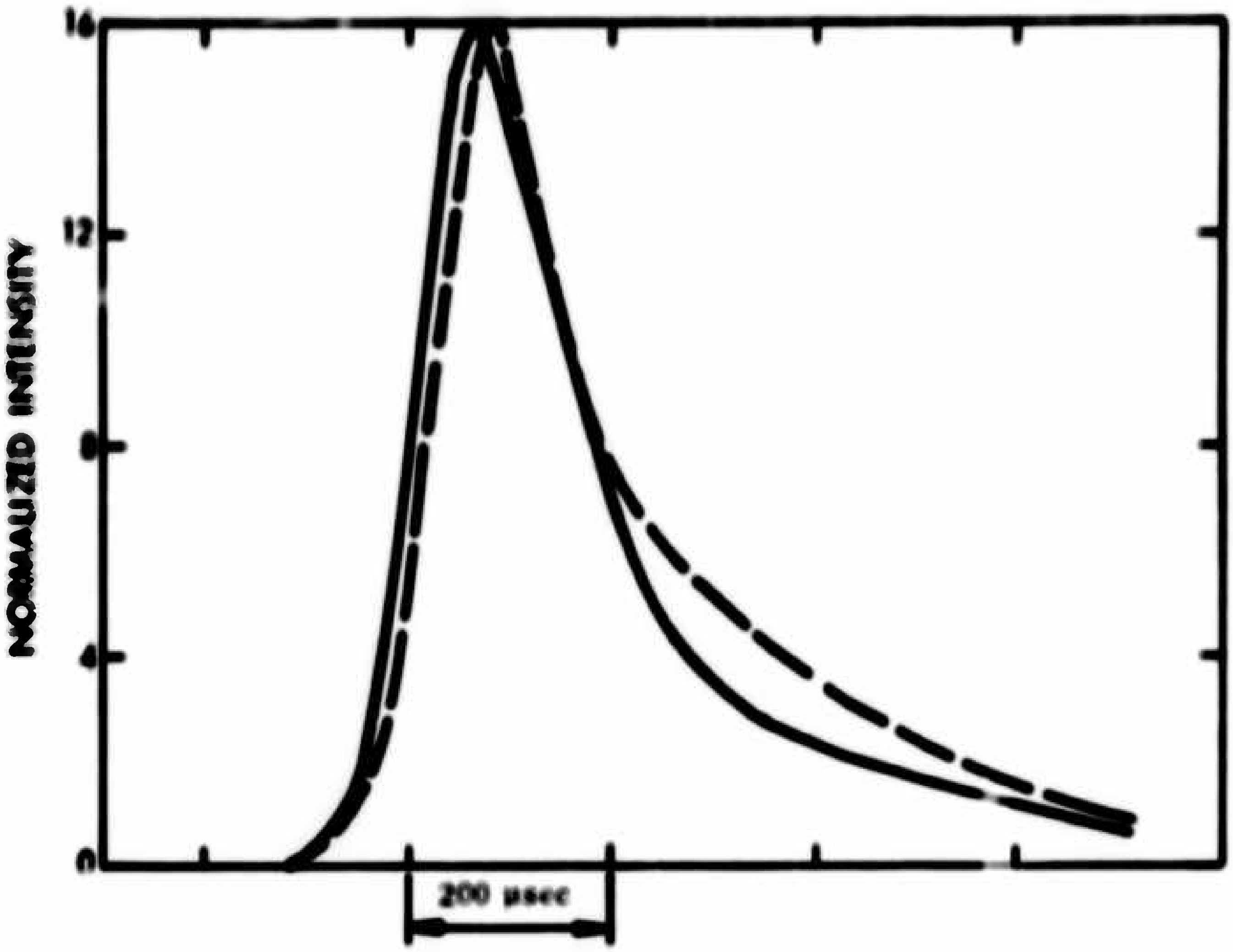

Figure 21 - Time-of-Arrival Behavior of a Chopped Beam of Carbon Vapor. Comparison of 36^+ at 50 eV versus 17.7 eV electron energy. Time scale relative to same photocell trigger in each case. Dashed curve is at 50 eV. Ion Source No. 1.

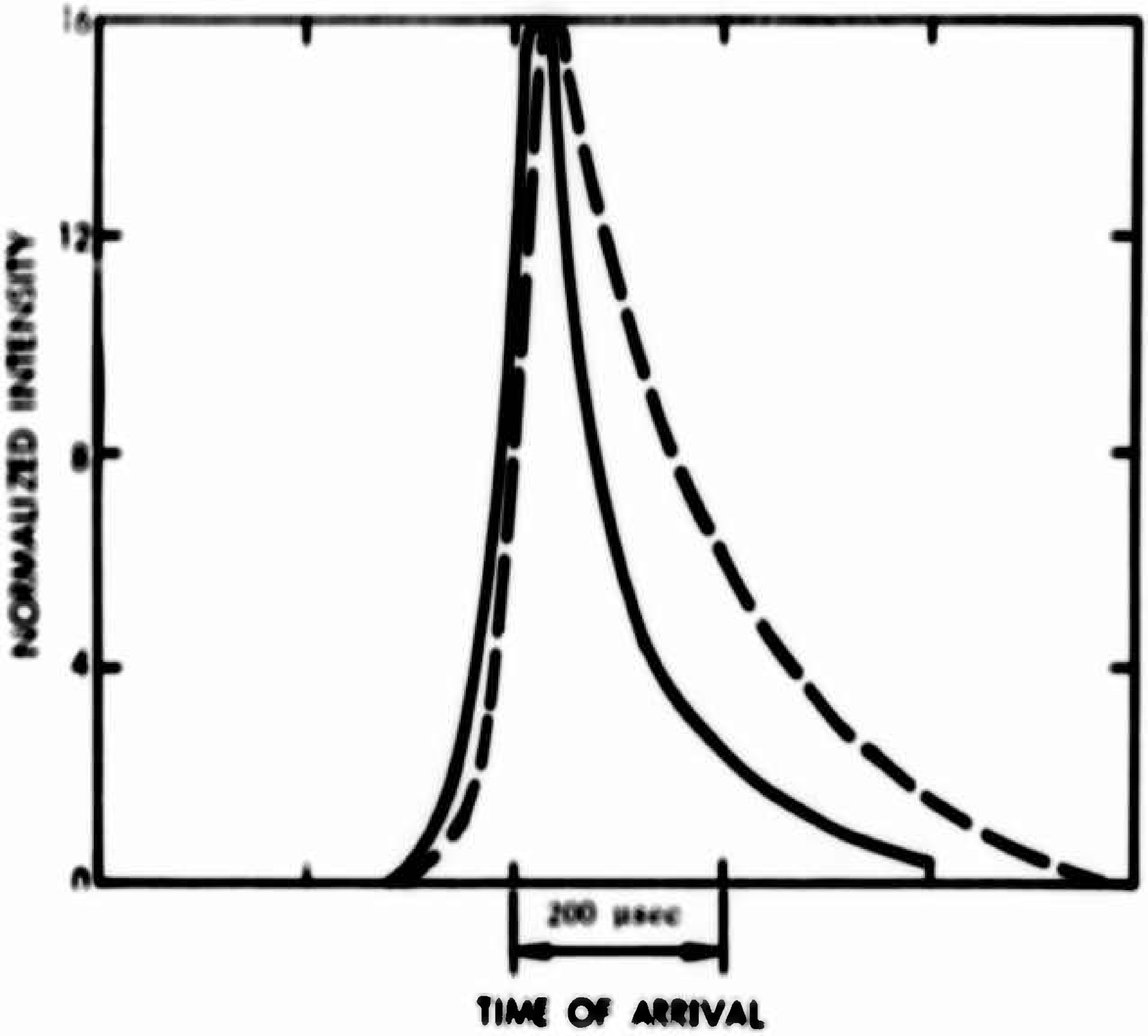

Figure 22 - Time-of-Arrival Behavior of a Chopped Beam of Carbon Vapor. Comparison of 12^+ at 50 eV versus 17.7 eV electron energy. Time scale relative to same photocell trigger in each case. Dashed curve is at 50 eV. Ion Source No. 1.

TABLE VIII

BEHAVIOR OF TIME-OF-ARRIVAL CURVES FOR CARBON SPECIES AS A FUNCTION OF ELECTRON ENERGY AND EMISSION CURRENT. ION SOURCE NO. 2.

Carbon Evaporation Conditions	Ion	Emission Current	Electron Energy	Time to Peak Intensity (arbitrary time in μsec)	Width at Half Maximum Intensity (μsec)
ATJ, Graphite Free Evaporation	36^+	2.0	17.7	X + 134	179
		2.0	50.0	X + 204	282
	24^+	2.0	17.7	X + 70	141
		2.0	50.0	X + 134	250
	12^+	2.0	17.7	X	141
		2.0	50.0	X + 64	218
Pyrolytic Graphite, Free Evaporation	36^+	2.0	14.0	X	167
		2.0	15.0	X + 7	192
		2.0	17.7	X + 13	192
		2.0	25.0	X + 26	179
		2.0	40.0	X + 77	230
		2.0	50.0	X + 103	243
		2.0	100.0	X + 359	359
		1.0	40.0	X + 333	333
		0.5	40.0	X + 449	320

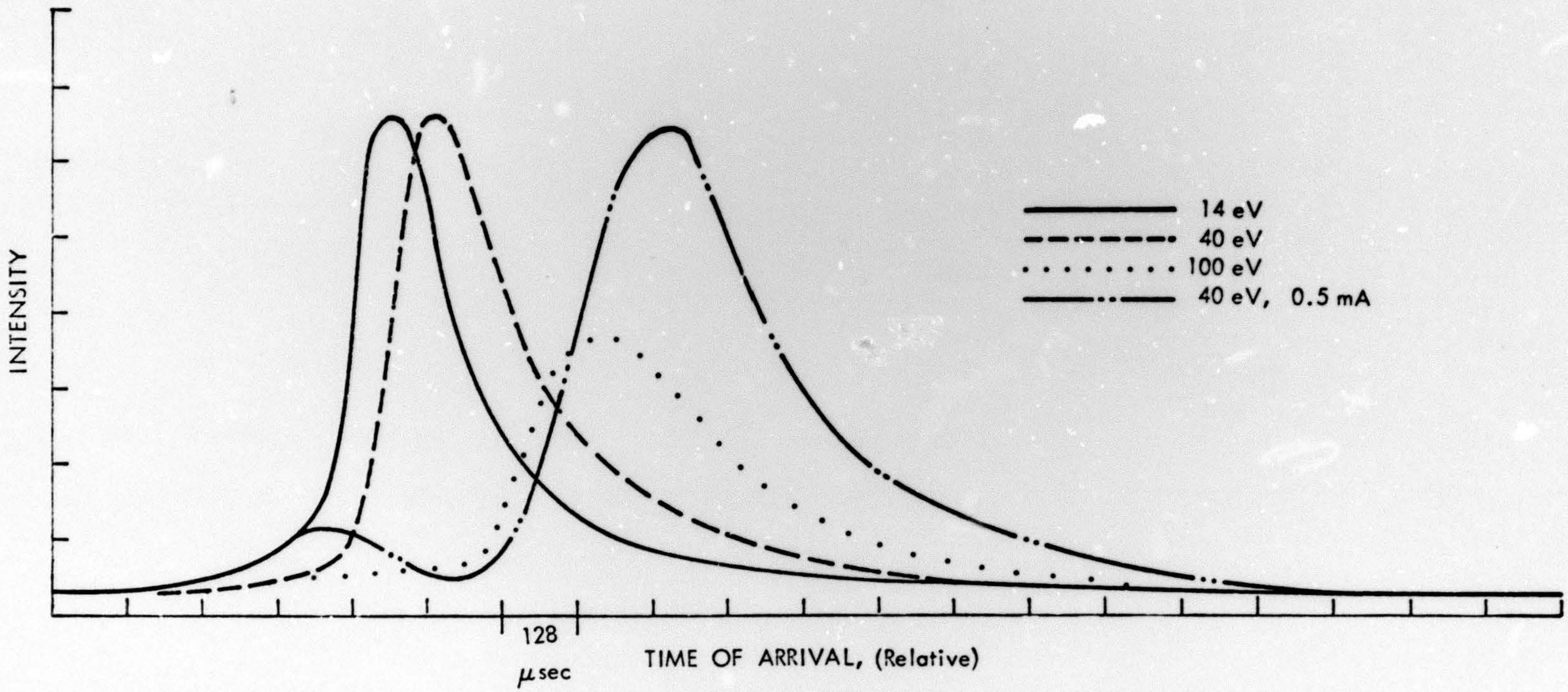

Figure 23 - Apparent Time-of-Arrival Behavior for C_3^+ From Free Evaporation of Pyrolytic Graphite, as a Function of Electron Energy and Emission Current. Curves not normalized in intensity. Ion Source No. 2.

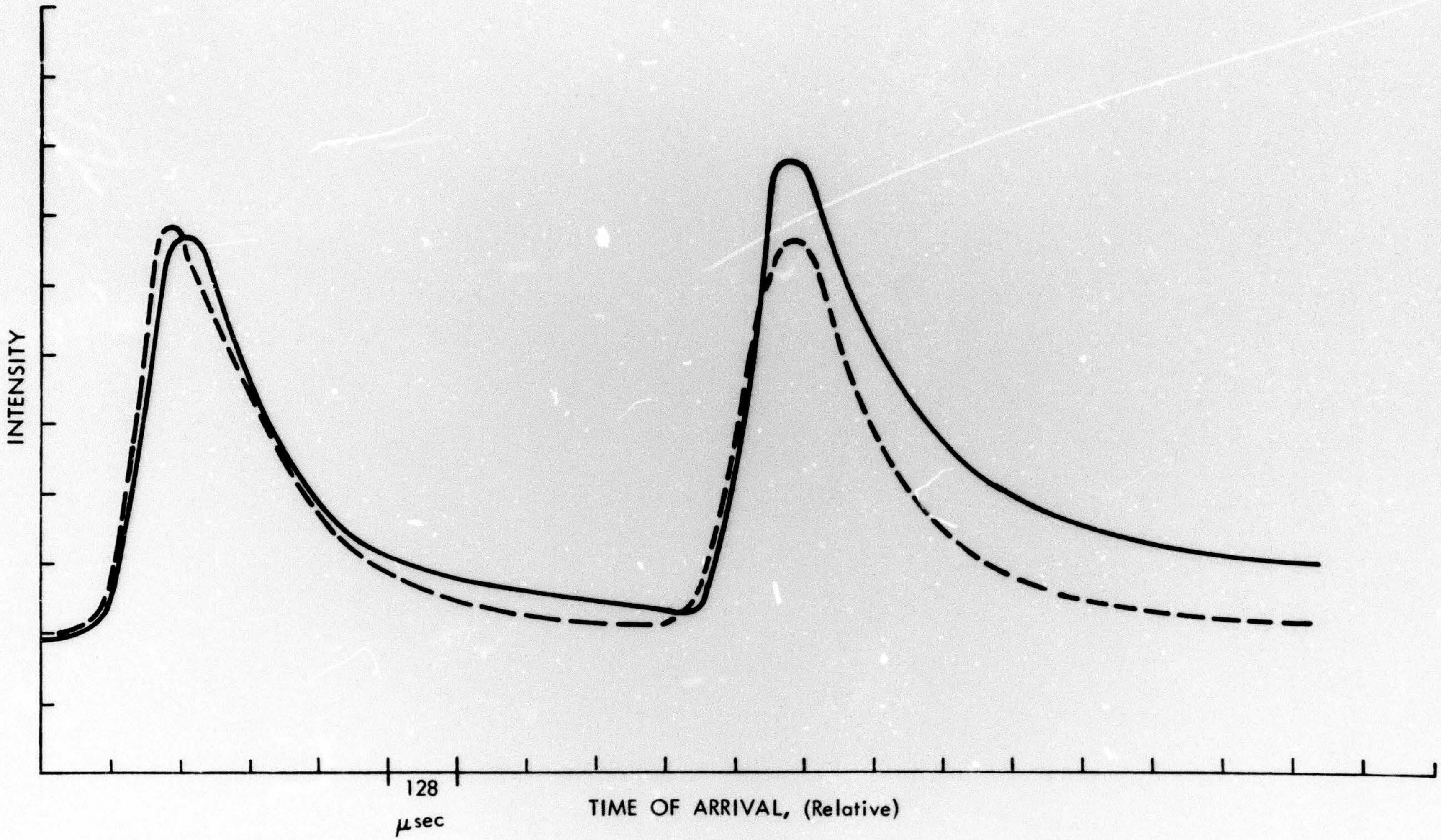

Figure 24 - Apparent Time-of-Arrival Behavior for C_3^+ From Free Evaporation of ATJ Graphite, as a Function of Electron Energy. Dashed curve 2 mA, 50 eV. Solid curve 2 mA, 100 eV. Ion Source No. 3

2. Continuum effects. An additional comment can be made relative to the correlations of dimer growth shown in Figure 14, p. 32 of Ref. 2. Herschback et al. (Ref. 15) have recently observed dimerization in Cs at 700°-800°K and if the excess dimer formed is plotted versus $P_o^2 d$, it appears that a mole fraction of about 10^{-2} is reached already at 0.4 torr^2 in. while 10^{-1} is reached at 40 torr^2 in. These results thus continue the trend toward faster nucleation rates the more strongly bound the dimer and reinforce the concern voiced in Ref. 2, p. 31, namely that some past Knudsen cell studies and laser evaporations may have been influenced by clustering during vapor expansion to collisionless flow.

IV.

SIGNIFICANCE OF THE RESEARCH FOR THE DESIGNER

In recent analytical descriptions of graphite ablation, lack of direct experimental characterization has forced rather widely varying limiting cases to be assumed. Thus, the sublimation process has been viewed as in equilibrium at the wall or as kinetically controlled. In addition, the contributions of preferential evaporation and oxidation to bulk removal of graphite grains has been considered. In the case of the equilibrium predictions, not the least of the problems involves the large uncertainties in both heat and entropies for carbon species larger than C_2. Reliable partition functions for C_3 are not available even though the fundamental vibrational frequencies are known. The heat of formation of C_3 is also still in major doubt. Estimates of thermodynamic properties for higher clusters are all based heavily on C_3 to compound uncertainties. Extrapolations from present experimental temperature limits of about 3200°K are also extreme.

In the case of kinetically controlled evaporation, evaporation coefficients are quite uncertain for clusters beyond C_3, even for well defined surfaces, not to mention the real case of highly pitted and porous surface conditions. Since no knowledge exists of reaction rates among carbon species, once evaporated, such reactions are usually ignored. The problem of particulate removal is equally complex and has been studied most thoroughly by Aerospace personnel. This research is not aimed directly at elucidating this aspect of real ablation behavior.

What does appear to be needed, in modeling the first two limiting cases, is direct experimental information on species ratios in equilibrium and free evaporation at substantially higher temperatures and pressures than the current limit of about 3200°K. Third-law determinations of heats of formation appear unreliable for clusters larger than C_3 in view of problems with partition functions including uncertainties in electronic states. Thus, the best approach appears to be to measure the temperature dependence of ion ratios relative to the well known C_1 and C_2 under both equilibrium and "free" evaporation conditions, realizing the latter are particularly ill defined. Whether heats can be inferred from such measurements will depend on resolving questions of temperature dependent cross sections, fragmentation contributions to a given ion and perturbations by gas phase reactions following vaporization. The latter information on carbon cluster reactions, which will emerge automatically in demonstrating the reliability of vaporization data, could prove useful in modeling behavior in boundary layers, particularly if the carbon vaporization is kinetically controlled.

At the very least, direct observations of carbon cluster ratios to temperatures approaching 3700°K and comparisons of equilibrium versus "free" evaporation ratios, no matter how ambiguous the latter, will help to substantially reduce the range of theoretical carbon species ratios currently used as input in calculated carbon vaporization predictions.

V.

FUTURE WORK

The fourth year's research can be summarized in terms of several restrictions and goals. First, we will concentrate on vaporization studies in vacuum. Second, we will look at both equilibrium and "free" evaporation of graphite. Third, emphasis will be placed primarily on gathering data on species beyond C_3 and on temperatures between 3200°K and 3700°K. Realizing that equilibrium pressures approaching a few tenths of an atmosphere may exist at 3700°K, and that mass loss could be of the order of a few tenths of a gram per second per square centimeter, one can readily surmise the difficulty and limited duration of vacuum heating to 3700°K. Fourth, time-of-arrival velocity analysis will be used routinely to supplement the information on temperature of the source vapor, to establish the neutral precursors of the ions studied and to detect the onset of continuum expansion effects which could lead to mass separation and clustering and thus to an overemphasis of the heavier carbon molecules.

A. Equilibrium Studies

The apparatus will be essentially as described above. We will use slotted PG cylinders and lids to act as radiation shields and to prevent vapor loss from the inductively heated carbon cells. Knudsen cells of PG, ATJ or other materials can be inserted in the PG. Temperatures will be read through the top laser port by means of a manual optical pyrometer. A moveable film viewing port perhaps mechanically driven will serve to keep carbon deposits from invalidating readings during vaporization. For short duration runs, a simple photocell system may be set up to monitor relative heating histories with the optical pyrometer serving for point calibration purposes. In a typical experiment, with the peak switcher preset on, say, C_3^+ and C_5^+ the RF power will be set to some preselected value destined to cause heating to, say, 3500°K. Over the heating period, the phase locked intensities of the two peaks will be alternately monitored and the time-intensity behavior stored in the multichannel analyzer or on a strip chart. Optical pyrometer readings and possibly photocell output can then be time-correlated with the stored mass spectral data. By repeat heatings involving the same temperature excursion, other ions relative to C_3^+ (or some other standard ion such as C_1^+) can be followed, ultimately yielding the composition-temperature behavior for the evaporation conditions chosen. An attempt will be made to obtain detailed information on species through C_9^+ at temperatures approaching 3700°K.

To verify temperatures, to check on continuum expansion perturbations or to assess the contribution of dissociative ionization to a given observed ion, the temperature will be quickly raised to a constant, chosen level and TOA curves rapidly run off in the four memory quarters available to us in the multichannel analyzer.

It is hoped that by aligning the beam defining slits carefully only vapor originating from the interior of the cell will enter the ion source. Of course, as pressures rise collisions will begin to occur outside the orifice and vapor from external surface evaporation, or from walls of the orifice, can collide with the interior vapor and alter its composition. The highly anisotropic nature of PG gives hope that such exterior evaporation can be kept to a tolerable level and allow implementation of the self-contained Knudsen cell approach to carbon.

From species-versus-temperature data obtained as just described one expects to get free energies from ion ratios and heats from temperature variation of these ratios.

B. Free Evaporation Studies

These studies will be identical to the equlibrium measurements except that no cavity will exist in the inner graphite susceptor, so that material "freely" evaporating from the surface can be directly monitored. Several types of graphite, including PG and ATJ, will be examined. Quite apart from the recognized problems of defining a unique "free" evaporation behavior for a heterogeneous substance such as graphite, whose surface morphology changes with time and which emits particulate matter, there is another problem as temperatures and pressures rise. At sufficiently high evaporation rates, gas phase collisions will be extensive immediately above the surface and composition may change during the escape of vapor from the surface. Thus this "free" evaporation behavior may depend on the size of the evaporating specimen as well as other factors. The time-of-flight techniques used to detect continuum expansion effects in equilibrium studies will serve equally well to observe such effects during "free" evaporation. At the very least, we can observe the gross molecular composition of vapor far downstream of the surface in "free" evaporation. Such information should be useful in comparison with equilibrium studies and for design purposes even though the detailed factors affecting the composition, such as the nature of the surface and its change with time are not uniquely specified.

C. TOA Analysis of Chopped Beams

Time-of-arrival analysis of chopped carbon vapor beams will be used routinely to help characterize the vaporization process and the mass spectra. Under Knudsen effusion conditions, most probable velocities can be related to source temperature for species of known molecular weight and hence source temperatures can be inferred. This measurement could prove particularly valuable for free evaporation studies where surface temperatures can be ambiguous due to emissivity uncertainties. Velocity distribution analysis is expected to reveal whether more than one parent is contributing to a given ion under chosen conditions. Ideally, the use of such analysis gives a molecular weight spectrum of the carbon vapor independent of the particular fragmentation behavior of the molecules involved. Both of these uses of velocity analysis are greatly complicated as collisions begin to occur during vapor expansion either from the Knudsen cell orifices or a free surface and hence will be most productive at the lower pressures.

An important secondary task, to validate the data being obtained, will be to search for the conditions of onset of continuum expansion effects and the resulting species velocity perturbations. Continuum effects, in addition to obscuring temperature measurement and neutral precursor determination, can lead to errors in cluster distribution determination, both through mass separation and clustering reactions.

REFERENCES

1. Milne, T. A., F. T. Greene, S. L. Bennett, and J. E. Beachey, AFML-TR-69-225, November 1969, "Mass Spectrometric Studies of Graphite Vaporization at High Temperatures," Contract No. F33615-68-C-1709.

2. Milne, T. A., F. T. Greene, and S. L. Bennett, "Mass Spectrometer Studies of Graphite Vaporization at High Temperatures," Technical Report AFML-TR-70-192, 1 July 1969 - 30 June 1970, Contract No. F33615-68-C-1709.

3. Unpublished notes from "Workshop for Graphite Ablation," held March 25-26, 1971, at the Aerospace Corporation, El Segundo, California.

4. Clark, J. T., and B. R. Fox, J. Chem. Phys., **51**, 3231 (1969).

5. Steele, W. C., "Studies of Graphite Vaporization Using a Modulated Beam Mass Spectrometer," Technical Report, AFML-TR-70-67, March 1970.

6. Wachi, F. M., and D. E. Gilmartin, Carbon, **8**, 141 (1970).

7. Williams, C. H., Paper presented at the Eighteenth Annual Conference on Mass Spectrometry and Allied Topics, San Francisco, June 14, 1970.

8. Zavitsanos, P. D., Final Report prepared for Sandia Laboratories, Revised June 1970, Contract No. AT(929-1)-789.

9. Moore, A. W., A. R. Ubbelohde, and D. A. Young, Brit. J. Appl. Phys., **13**, 393 (1962)

10. Storms, E., Los Alamos Scientific Laboratory, private communication.

11. Greene, F. T., and T. A. Milne, "An Experimental Study of the Structure, Thermodynamics and Kinetic Behavior of Water," Contract No. 14-01-0001-1479, Office of Saline Water.

12. Anderson, J. B., and J. B. Fenn, Phys. of Fluids, **8**, 780 (1965).

13. Kaufman, M. J., Princeton University, private communication.

14. Storms, E., and R. Hall, Los Alamos Scientific Laboratory, private communication.

15. Gordon, R. J., Y. T. Lee, and D. R. Herschback, J. Chem. Phys., **54**, 2393 (1971).

Preceding page blank

APPENDIX

The following comments on the ion source behavior noted in this report have been supplied by Nuclide Corporation:

"The three types of ionizers (unmodified) described in this report represent successive steps by Nuclide in a continuing program to develop a better ion source for the study of steady molecular beams diffusing continuously from Knudsen cells at constant temperature. While sources of all three types had been used routinely with manually operated molecular beam shutters for many years, none of them had been tested in a pulsed beam application by Nuclide or, to our knowledge, by any other users, until the experiments described in this report. The new information obtained here should therefore be generally applicable to this entire class of ion sources, which are used in numerous laboratories throughout the world. These authors report that the Nuclide source of most recent design (referred to as "Source No. 3" in this report), which is a source that does not use a magnetic field for electron collimation, had produced the best overall results in their experiments, in this particular instrument. However, they find this source to be considerably less sensitive than "Source No. 1", also a "nonmagnetic" source, and to have about the same sensitivity as the Nuclide source which utilizes a magnetic field for electron collimation. On the other hand, certain other 12-90-HT users have reported that the "Nuclide magnetic ion source", as used in their particular instruments and experiments, is in fact more sensitive than nonmagnetic "Source No. 1". Tests of sensitivity in terms of the minimum detectable partial pressure of a silver isotope in a Knudsen cell are routinely performed by Nuclide during both in-plant and installation testing. All three types of sources have demonstrated the ability to detect a partial pressure of less than 2.5×10^{-8} torr for a silver isotope, in different instruments but under similar operating conditions. It is our opinion, based on such tests, that the sensitivities of these three types of sources are identical to within perhaps a factor of two to three, the limit of error of the measurement."

The discrepancy between the relative sensitivities reported in Table II and those cited above based on Nuclide experience remains unresolved. We hope that on rechecking, Ion Source No. 3 will compare more favorably with Source No. 1.

Preceding page blank

It should be emphasized that the background modulation phenomenon, so easily detectable with chopped beams, is also of concern in conventional Knudsen cell, steady-beam arrangements when manual shuttering is used. We have observed changes in background peak intensitires, using ion-source No. 1, when Knudsen beams are manually shuttered.